Kidney and Adrenal Gland

13

Xiaohua Qian

The Kidney

Introduction

Fine-needle aspiration (FNA) biopsy of the kidney is a valuable diagnostic modality for radiographically indeterminate mass lesions, for workup of systemic diseases (metastasis, lymphoma, or infection), and for establishing a malignant diagnosis in nonsurgical candidates. Recent advances in imaging, interventional radiology, and cytologic ancillary techniques have enhanced the accuracy of renal FNA [1–3]. Judicious application of immunohistochemistry and genetic/molecular techniques has made subclassification of renal neoplasms possible in FNA samples [4].

Indications for Renal FNA

- Radiological findings are inconclusive:
  - Cystic lesions, small solid masses, and bilateral masses
- Radical nephrectomy is contraindicated:
  - Unresectable renal cell carcinoma (RCC)
  - Possible metastatic tumor
  - Possible lymphoma
  - Patient with significant comorbidities
- Partial nephrectomy is indicated.
- Cryoablation therapy is indicated.
- Infection is suspected.

Specimen Collection and Preparation

FNA biopsy of renal masses is now most often performed percutaneously by radiologists using computed tomography (CT), less commonly ultrasonography (US), and rarely magnetic resonance imaging (MRI) guidance. Slides are air-dried and stained with Diff-Quik (DQ) and/or alcohol-fixed and stained with the Papanicolaou (Pap) or hematoxylin and eosin (H&E) stains. DQ and Pap stains are both helpful and complementary to each other. The DQ stain is valuable for on-site adequacy evaluation, which significantly increases the successful rate of needle biopsy [5]. It is also useful in assessment of cytoplasm texture, bringing up the papillary architecture and the cytoplasmic hyaline globules in certain types of epithelial renal tumors. Pap stain is helpful in delineating the nuclear details. Cell blocks and ThinPrep slides are useful for immunohistochemical studies. Cell blocks and core needle biopsies taken with a larger needle (18 gauge or larger) provide the benefit of tissue architectural features [6]. Immunohistochemical studies can be helpful in separating metastatic tumors from primary renal tumors and in subtyping renal epithelial cell neoplasms in some settings. There is, however, considerable overlap between immunohistochemical expression among different renal cell carcinomas [7]. Therefore, results of a panel of markers must be interpreted in conjunction with clinical presentation, cytomorphology, as well as molecular genetic information if available. Molecular cytogenetic techniques play an increasingly significant role in subtyping RCCs and confirming the diagnosis of certain types of mesenchymal tumors and lymphomas [2, 8].

Accuracy and Adequacy

Although renal FNA is a safe and accurate diagnostic modality with high sensitivity (75–92%) and specificity (91.9–99%) in experienced hands, the use of a combination of fine and larger needles has become a trend in many medical centers [6]. False-positive diagnoses commonly result from misinterpretation of benign hepatocytes, adrenal cortical cells, and normal renal parenchyma as a RCC or urothelial carcinoma. The most common false-negative diagnosis is a sampling error of a cystic RCC. In the contemporary era of frequent detection of small renal masses, the diagnostic accuracy of needle biopsy remains higher than 90% [3], albeit the rate of biopsy failures has increased as a result of inaccurately targeting the mass, especially the ones smaller than 1 cm [6]. Serious complications from needle biopsy are extremely rare; however, tumor infarction and hematoma have been reported [9].

X. Qian
Department of Pathology, Brigham & Women's Hospital, Harvard Medical School, 75 Francis Street, Boston 02115, MA, USA
e-mail: xqian@bwh.harvard.edu

H. A. Domanski (ed.), *Atlas of Fine Needle Aspiration Cytology*, https://doi.org/10.1007/978-3-319-76980-6_13

Normal Elements

Normal glomeruli and renal tubular cells appear on FNA smears when the biopsy needle inevitably traverses the normal kidney parenchyma, usually the renal cortex, and especially when a small, intraparenchymal lesion is targeted. It is extremely important not to overinterpret these normal elements as neoplastic cells.

Glomeruli and tubular cells often coexist in relatively hypocellular smears (see Fig. 13.1a). Glomeruli are densely cellular, multilayered, and lobulated globular clusters with capillary loops (see Fig. 13.1b). At scanning magnification, they mimic vascularized cellular clusters of papillary RCC and angiomyolipoma (AML).

Proximal tubular cells appear as small, loose clusters of epithelial cells with ill-defined cell borders, granular cytoplasm, and a bland round to oval nucleus with a small nucleolus (see Fig. 13.2a). Their appearances are similar to those of tumor cells in renal epithelial neoplasms with granular cytoplasm, such as oncocytoma, chromophobe RCC, and low-grade conventional RCC. Distal tubular cells are smaller, more cohesive, and with less and less granular cytoplasm than proximal tubular cells (see Fig. 13.2a). Occasionally, an intact distal tubule may be seen as a long, serpentine cast (see Fig. 13.2b). It can be sometimes quite challenging to distinguish normal renal tubular cells from tumor cells of a not well-sampled, low-grade renal epithelial neoplasm. A specimen containing only normal renal elements should be reported as nondiagnostic rather than negative for malignancy.

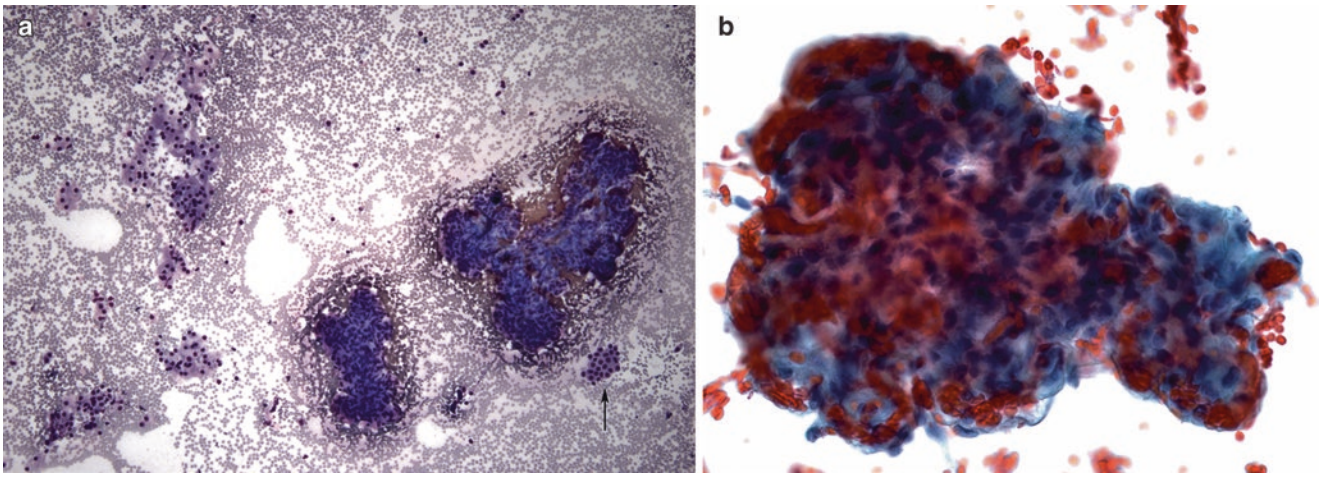

Fig. 13.1 Normal kidney elements. (**a**) Glomeruli (two lobulated structures, *right*) and tubular cells (proximal tubular cells, *left*; *arrow* indicates distal tubular cells) coexist in relatively hypocellular smears at scanning magnification (Diff-Quik stain). (**b**) Glomeruli characterized by densely cellular and lobulated globular clusters with capillary loops containing abundant red blood cells (Pap stain)

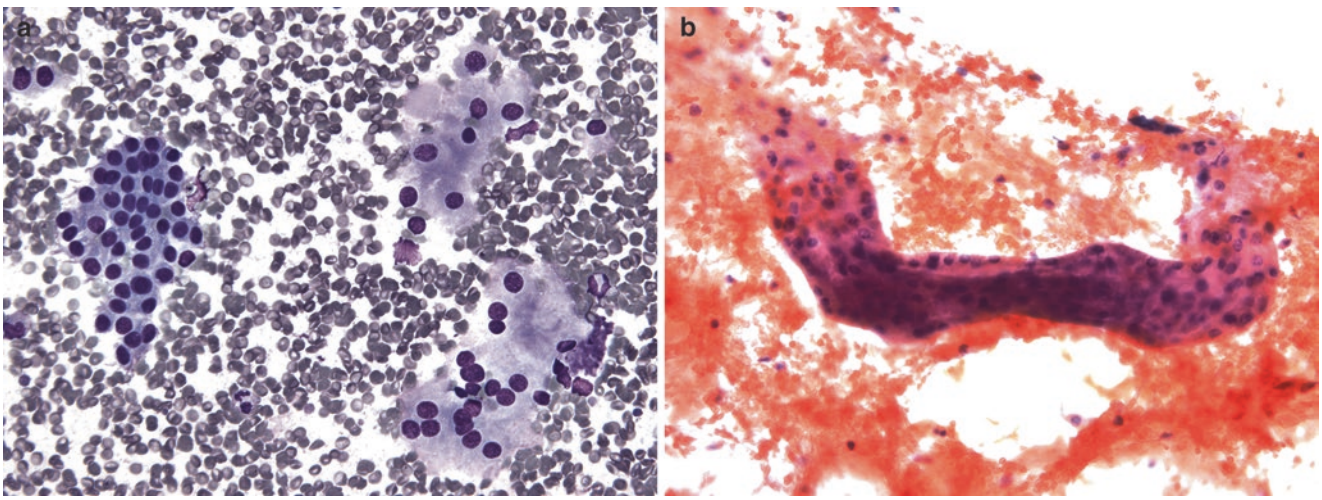

Fig. 13.2 Normal tubular elements. (**a**) Proximal tubular cells (right cluster) are small, loose clusters of epithelial cells with ill-defined cell borders; granular cytoplasm; and a bland round to oval nucleus; distal tubular cells (left cluster) are smaller, more cohesive epithelial cells with less and less granular cytoplasm than proximal tubular cells (DQ stain). (**b**) An intact distal tubular fragment shown as a long, serpentine cast (Pap stain)

Cystic Lesions

Renal cysts are among the most common mass-forming lesions identified radiographically. Most congenital cysts and other simple cysts are easily recognizable on imaging studies. Only radiologically atypical cysts, such as the ones with thickened septations and/or thick walls, are sometimes targets of FNA.

The smears are consistently hypocellular and contain variable number of histiocytes and macrophages (Fig. 13.3a). Liesegang rings, ball-like spherical structures with rads and concentric rings, can also be found in cyst fluids (Fig. 13.3b, c). Depending on the nature of cysts, few epithelial and/or stromal elements can also be present. Cystic nephroma, a benign multilocular cystic neoplasm, is now considered as a part of the spectrum of renal epithelial and stromal tumor (REST) [10]. They often yield reactive epithelial cells and/or spindled stromal cells (often ovarian-like), which could be mistaken for cystic RCC or angiomyolipoma or even sarcoma. Cystic clear-cell RCC, especially a low-grade tumor, can yield only a few deceptively bland neoplastic cells (Fig. 13.4) and is conceivably a major cause of false-negative diagnosis.

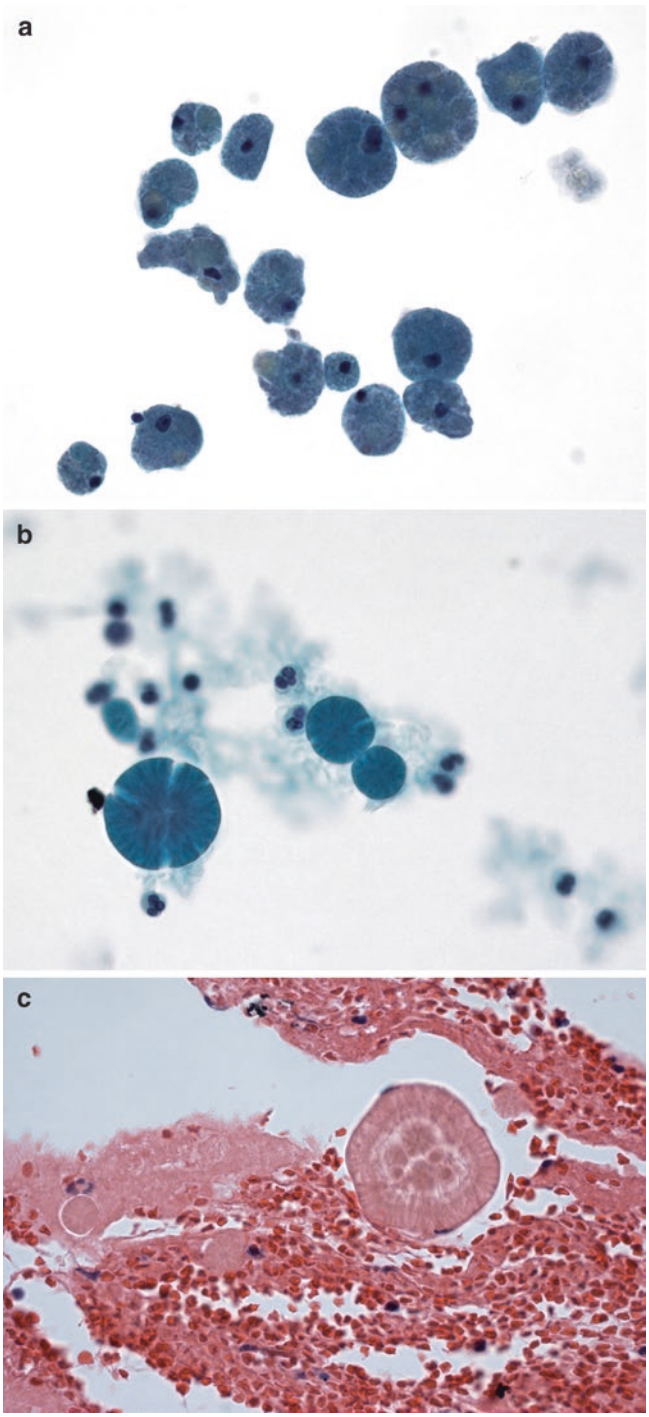

Fig. 13.3 Cyst contents. (**a**) Macrophages are common findings of all cystic lesions including renal cysts. (**b**) Liesegang rings are ball-like spherical structures in variable sizes with crystallite-like rays from a central core and concentric rings (ThinPrep, Pap stain), which are better appreciated on cross section in cell block material (**c** H&E stain)

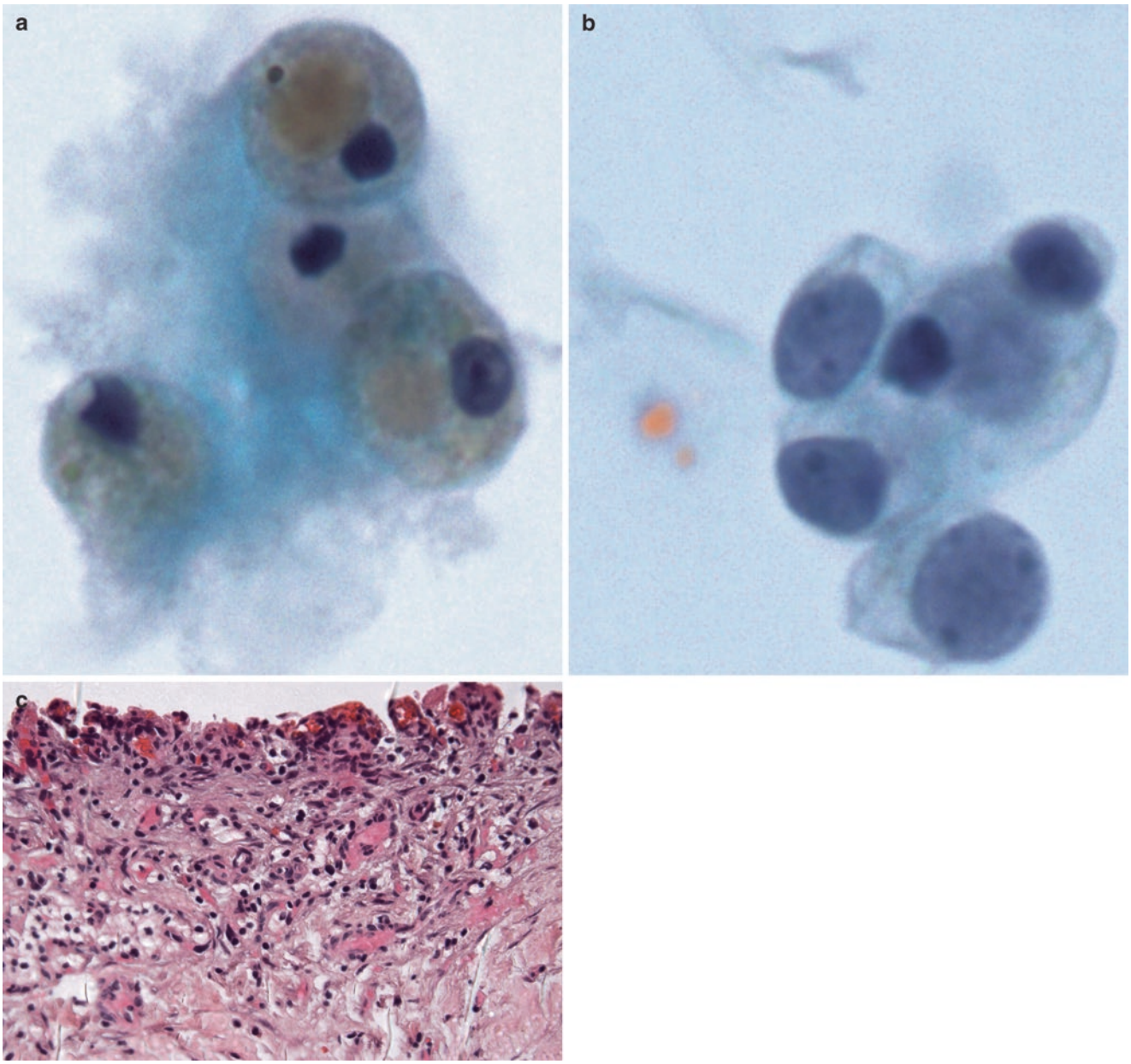

Fig. 13.4 Cystic RCC. (**a**) Abundant macrophages in cystic RCC can be misleading. (**b**) Rare groups of epithelial cells with slightly enlarged nuclei (compared to the macrophage nuclei) and clear cytoplasm can be easily overlooked (Pap stain). (**c**) Corresponding histologic section showing partially denuded cyst wall lined and superficially infiltrated by same low-grade clear-cell RCC tumor cells (H&E)

Benign Lesions

Oncocytoma

Oncocytoma is a benign tumor of oncocytes (large epithelial cells with mitochondria-rich granular cytoplasm), comprising approximately 5% of all renal tumors. It occurs more frequently in men, with a peak incidence in the seventh decade of life [11]. Because of the lack of its typical central scarring appearance on image studies in some cases, oncocytoma is often targeted for FNA.

Aspirates are usually at least moderately cellular, composed predominantly of isolated cells, loose small clusters, and occasional large tissue fragments (Fig. 13.5a). The oncocytes vary in size and are uniformly of polygonal shape. Their distinctive features include well-defined cell borders, abundant granular cytoplasm, and round, eccentrically located nuclei with prominent nucleoli, like pomegranate seeds (Fig. 13.5b). Binucleation and nuclear pleomorphism are not uncommon. The nested architecture of tumor cells (Fig. 13.5c), a characteristic feature and a helpful clue of oncocytoma, can be appreciated sometimes on the cell block sections. The primary differential diagnosis is chromophobe RCC. Nested tumor cells, round nucleus, and lack of perinuclear halo favor oncocytoma. In difficult cases, Hale's colloidal iron stain would be helpful: oncocytomas show negative reaction or focal apical positive reaction (Fig. 13.5d). In contrast, chromophobe RCCs show a diffuse positivity (Fig. 13.11e). A positive S-100A1 immunostain also supports the diagnosis of oncocytoma; however, a negative staining in a small biopsy does not necessarily exclude the diagnosis since S-100A1 staining can be patchy (Fig. 13.5e) [12].

Cytologic features:

- Moderately cellular smears with predominantly isolated cells
- Polygonal cells in variable sizes
- Eccentrically located, often nucleolated, round nucleus, granular cytoplasm, and well-defined cell borders
- Binucleation
- Nested tumor cells on cell block

Differential diagnosis and problems in diagnosis:

- Chromophobe RCC
- Clear-cell RCC, granular cell variant
- Papillary RCC, type 2 subtype
- Tubulocystic RCC
- Inadvertently sampled hepatocytes

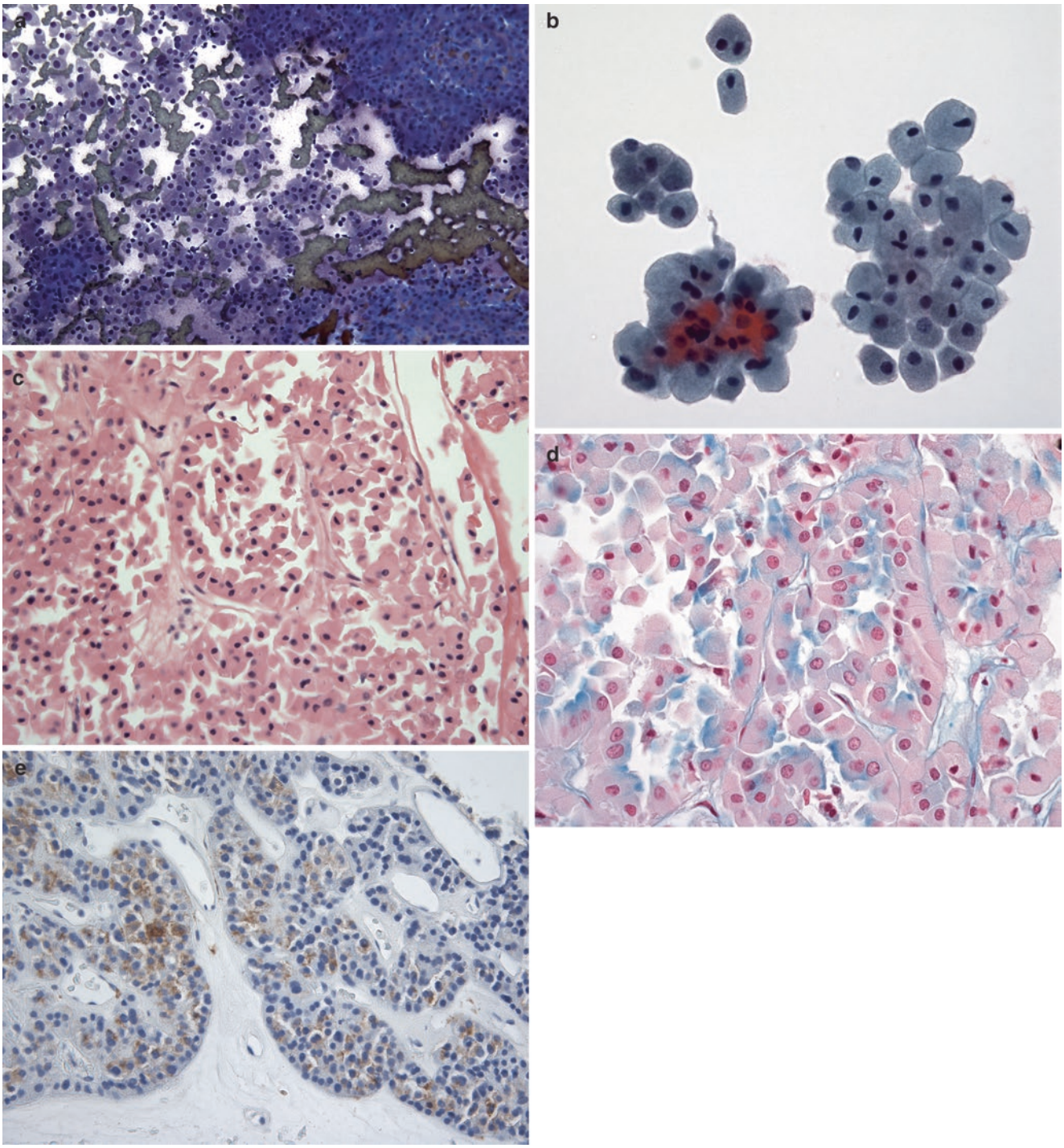

Fig. 13.5 Oncocytoma. (**a**) Scanning power shows a cellular smear with single cells, loose clusters, and large tissue fragments (DQ stain). (**b**) Polygonal cells in variable sizes, with eccentrically located nuclei, granular cytoplasm, and well-defined cell borders, reminiscent of pomegranate seeds (ThinPrep, Pap stain). (**c**) A nested architecture, with loosely cohesive tumor cells surrounded by thin capillaries, is best appreciated on cell block sections (H&E). (**d**) A Hale's colloidal iron stain showing an apical staining pattern. (**e**) A positive S-100 A1 staining (sometimes patchy) is helpful in supporting the diagnosis of oncocytoma

Angiomyolipoma

Angiomyolipoma (AML) is a benign mesenchymal tumor of the PEComa (perivascular epithelial cell) family. It occurs either as a sporadic, incidental lesion or in association with tuberous sclerosis. AML is typically composed of three elements: thick blood vessels, primitive smooth muscle cells, and mature adipose tissue. Since most AMLs can be reliably diagnosed by imaging studies based on the presence of their fat component, only the "fat-poor" AMLs, which are indistinguishable from a RCC radiologically, are subjected to FNA.

The smears are usually hypocellular but variable, with large jigsaw puzzle-like tissue fragments (Fig. 13.6a) composed of spindled to epithelioid smooth muscle cells in a syncytial appearance (Fig. 13.6b). The other two elements, thick-walled vessels (Fig. 13.6c) and mature adipose tissue, are less frequently present or even absent. These large cellular tissue fragments can be mistaken for papillary RCC, especially when there is some nuclear atypia [13] or epithelioid cells are predominant.

The positivity of both smooth muscle markers (SMA and/or desmin) and melanocytic markers (HMB-45 and/or Mart-1) is diagnostic for AML. Since HMB-45 immunoreactivity in AML could be patchy in histologic sections, lack of it in a small biopsy does not necessarily exclude AML.

Cytologic features:

- Variably cellular smears with jigsaw puzzle-like tissue fragments
- Cohesive cellular clusters with spindled to epithelioid cells
- Thick-walled vessels
- With or without mature adipose tissue

Differential diagnosis and problems in diagnosis:

- Papillary RCC
- Sarcomatoid RCC
- Dedifferentiated liposarcoma
- Fibrous capsular tissue

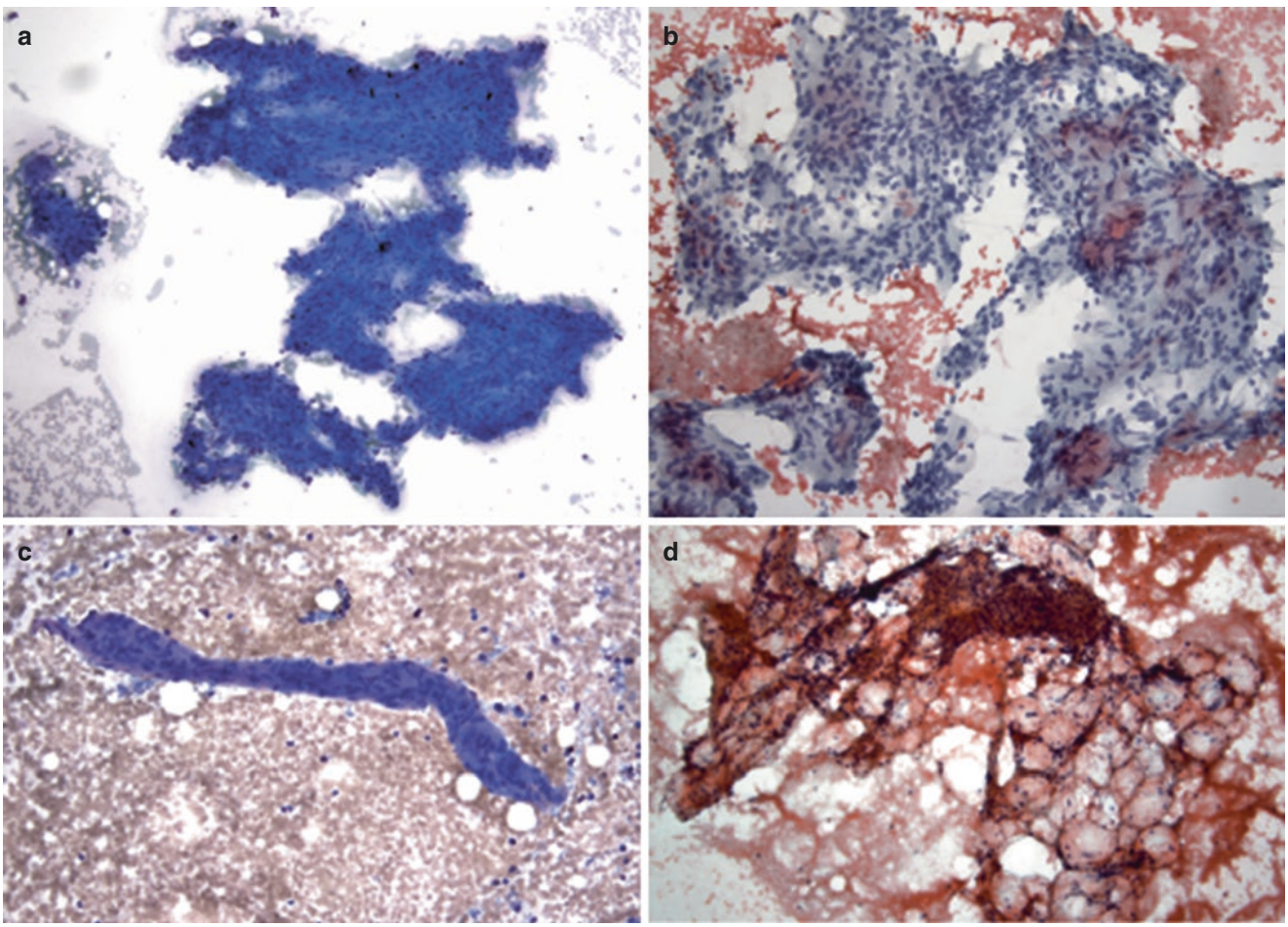

Fig. 13.6 Angiomyolipoma (AML). (**a**) Variably cellular smears with jigsaw puzzle-like tissue fragments (DQ stain). (**b**) Cohesive cellular clusters with bland spindled to epithelioid cells in a syncytial appearance (Pap stain). (**c**) Isolated or attached thick-walled vessels are occasionally present. (**d**) Mature adipose tissue, although likely absent due to sampling a fat-poor AML, intermingled with cellular areas of spindled cells, immediately suggests the diagnosis of AML

Metanephric Adenoma

Metanephric adenoma (MA) is a rare, benign renal epithelial neoplasm and commonly occurs in women in their 50s and 60s. These tumors are well circumscribed and range widely in size from a few centimeters to as large as 15 cm.

The aspirate smears are usually distinctive and show numerous short tubular structures and tight balls/acini, which are often attached to the ends of the tubules. These tubular or acinar structures are composed of tightly packed and uniformly bland cells, which have scant cytoplasm, ovoid nuclei with fine chromatin, and inconspicuous nucleoli (Fig. 13.7a–c). Psammoma bodies and stromal material may be present. Mitoses, nuclear atypia, and necrosis are usually absent [14, 15].

Cytologic features:

- Hypercellular smears with short tubular structures and tight balls/acini
- Tightly packed and uniformly bland cells with scant cytoplasm
- Occasional psammoma bodies

Differential diagnosis and problems in diagnosis:

- Papillary RCC, type 1
- Wilms' tumor (WT), epithelial/tubular dominant

In general, a panel of antibodies including WT-1, CK7, AMACR, CD57, and epithelial membrane antigen (EMA) would be sufficient to distinguish MA from papillary RCC and/or WT [16].

MA tumor cells are positive for WT-1 (Fig. 13.7d) and CD57 and negative for CK7, EMA, and AMACR, which distinguishes MA from papillary RCCs.

Most Wilms' tumors (WT) have a triphasic pattern, characterized by blastemal cells (small, blue, and mitotically active cells), an epithelial component, and areas showing mesenchymal differentiation. Only the WTs with prominent epithelial differentiation would enter the differential of MA. Although both MAs and WTs show nuclear expression of WT-1, their patterns of expression, however, are different: MA shows strong, diffuse staining, whereas WT shows variable staining depending on the areas of differentiation [17].

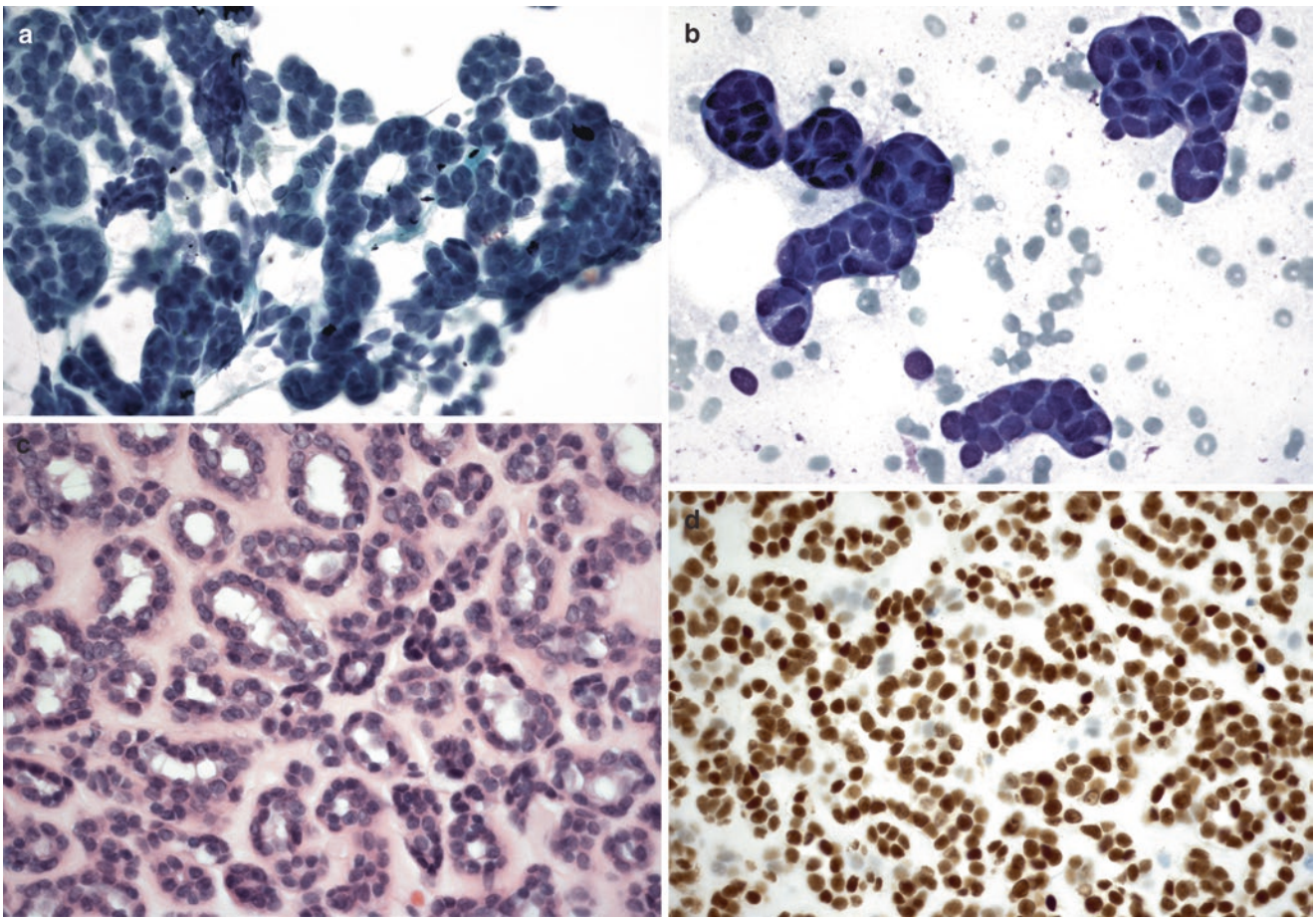

Fig. 13.7 Metanephric adenoma. (**a**, **b**) Cellular smears showing distinctive short tubular structures and tight balls/acini lined by uniformly bland cells with scant cytoplasm (**a** Pap stain; **b** DQ). (**c**) Numerous small tubular/acini structures embedded in a hyalinized stroma, best seen in cell block material (H&E). (**d**) A strong and diffuse immunostaining pattern for WT-1 is characteristic

Xanthogranulomatous Pyelonephritis

Xanthogranulomatous pyelonephritis (XPN) is an atypical host response to an upper urinary tract bacterial infection, and it may present as a renal mass radiologically. The abundant foamy histiocytes, especially in aggregates, can be confused with the cells of clear-cell RCC. The degenerated renal tubular cells may mimic cells from oncocytoma [18]. The FNA appearance of XPN is more inflammatory and lacks nuclear atypia (Fig. 13.8). The histiocytic nature of the lesional cells of XPN can be confirmed by immunoreactivity for CD163/CD68 in difficult cases [19].

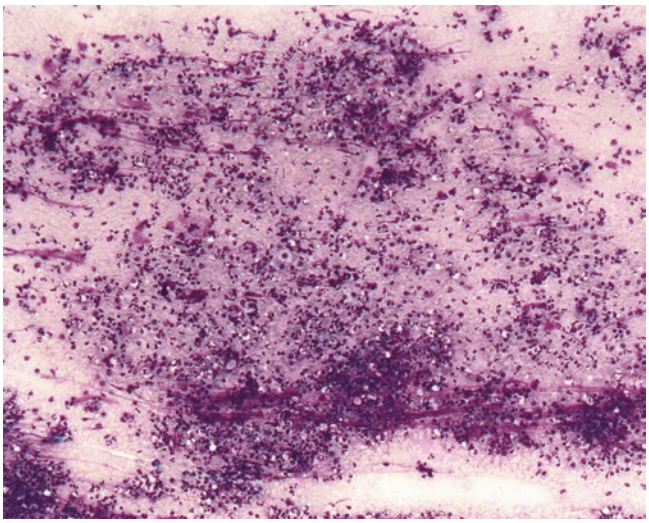

Fig. 13.8 Xanthogranulomatous pyelonephritis. Cellular smear showing predominantly inflammatory cells with admixed foamy histiocytes and degenerated epithelial cells. Note that nuclear atypia is absent (MGG stain; *courtesy of* Jerzy Klijanienko, MD, Institut Curie, Paris, France)

Malignant Neoplasms

Renal Cell Carcinoma

RCC is a malignancy of the renal tubules and represents more than 90% of all malignancies of the kidney in adults. Men are more commonly affected, and the incidence is higher in industrialized countries than in developing countries. Its risk increases with tobacco smoking, arsenic exposure, and obesity [20].

A minority of RCCs develop in the background of hereditary cancer syndromes or end-stage renal disease. The specific forms of hereditary RCCs include von Hippel–Lindau (VHL) clear-cell carcinoma, hereditary papillary renal carcinoma (HPRC), Birt–Hogg–Dube oncocytic neoplasm, and hereditary leiomyomatosis RCC [21]. The two distinctive novel tumors linked to end-stage renal diseases are acquired cystic disease-associated RCC and clear-cell papillary RCC [22].

Since approximately one third of patients with RCC present with metastases and solitary metastasis at unusual sites (e.g., thyroid, salivary glands, pancreas (see Fig. 4.36)) is common, it is essential to be familiar with the cytomorphologic spectrum of each subtype of RCC for accurate diagnosis of metastatic RCCs. Precise subclassification of RCC is also becoming increasingly important as effective molecular-targeted therapies are being developed for specific types of RCC.

The latest World Health Organization classification of renal carcinomas (2016) highlights the close relationship between the morphology and genetic abnormalities of each clinically distinct subtype of renal carcinoma [23, 24]. Notably, several distinctive forms of RCC, including hereditary leiomyomatosis and renal cell carcinoma syndrome-associated RCC, succinate dehydrogenase-deficient RCC, tubulocystic RCC, acquired cystic disease-associated RCC, and clear-cell papillary RCC are newly recognized in WHO 2016 [22, 25–27].

The Fuhrman nuclear grade is widely used in histology as one of the prognostic parameters, but nuclear grading in FNA or core needle biopsies remains controversial. Undergrading and interobservant variability are common caveats [28].

The following subtypes of malignant renal epithelial neoplasms are discussed below. Their cytogenetic abnormalities and immunoprofiles, which can be used to facilitate subclassification, are summarized in Table 13.1.

- Clear-cell (conventional) RCC
- Papillary RCC
- Chromophobe RCC
- Sarcomatoid RCC
- Renal translocation carcinoma
- Mucinous tubular and spindle cell carcinoma
- Collecting duct carcinoma (Bellini tumor)
- Clear-cell papillary RCC

Table 13.1 Cytogenetics and immunoprofile of selected renal epithelial neoplasms

RCC subtype	Cytogenetics	Immunoprofile[a]
Conventional/clear-cell RCC	Del 3p	RCC+/CD10+/AMACR+/CA IX+ (boxlike)
		CK7–/CD117–
Papillary RCC	Trisomies 7, 17	CK7+/AMACR+/CD10+
	Loss of Y	CD117–
Chromophobe RCC	Multiple losses	CD117+/CK7+
	−1, −2, −6, −10, −13, −17, −21	AMACR–
Translocation RCC		RCC+/CD10+/AMACR+
Xp11.2 translocation	*t*(X;1)(p11.2;q21) or *t*(X;17)(p11.2;q25)	EMA–/CK7–
		TFE3+
t(6;11)(p21;q12)	*t*(6;11)(p21;q12)	TFEB+
MTSCC	Multiple losses/gains[b]	CK7+/AMACR+
		CD10–/CD117–
Oncocytoma	11q13 involvement	S–100A1+/CD117+
	Loss of Y, X, or 1	AMACR–/CK7– or weak
Collecting duct carcinoma	Deletions: 1q, 6p,8p, 13q, 21q	CK7+/P63+
		RCC−/CD10−/AMACR−
Clear-cell papillary RCC	N/A	CK7+ CA IX + (cuplike) AMACR-/CD117-/CD10-

MTSCC mucinous tubular and spindle cell carcinoma, *RCC* renal cell carcinoma
[a]All tumors are positive for renal epithelial markers PAX8 and PAX2
[b]Inconsistent results in the literature so far

Clear-Cell (Conventional) Renal Cell Carcinoma

Clear-cell (conventional) RCC accounts for approximately two thirds of all renal epithelial neoplasms. It is characterized histologically by large, clear, and/or granular tumor cells nested within a network of thin-walled blood vessels. Hemorrhage, necrosis, calcifications, and cystic degeneration are common. These features (hypervascularity and heterogeneity) account for its characteristic appearance on imaging studies and the typical bloody smears on FNAs.

The cellularity of aspirates is highly variable, ranging from cellular smears with clusters and sheets of tumor cells to merely only blood; in later cases, the tissue fragments can sometimes be recovered in cell block sections (Fig. 13.9d). Deeper level sectioning can be rewarding in getting the diagnostic tissue fragments in a bloody cell block. In cellular smears, tumor cells are commonly seen in association with transgressing blood vessels, which can mimic a papillary RCC (Fig. 13.9a, b). The tumor cells may also be displayed as single cells or in small clusters, sometimes arranged like a butterfly (Fig. 13.9c) or petals of flower. The tumor cells are often larger than normal tubular cells (at least 2×) with a lower nuclear-to-cytoplasmic (N/C) ratio. The distinctive features (i.e., abundant, clear to finely vacuolated cytoplasm, rich in glycogen and lipid) are best appreciated on the DQ stain (Fig. 13.9c). The cell borders are often irregular and indistinct. The often eccentrically located nuclei are round and contain a variable-sized nucleolus depending on the grade of tumor: the smaller nucleolus in low-grade tumors progressing to a prominent one in higher-grade tumors. With the presence of all characteristic features, diagnosing clear-cell RCC based on cytomorphologic alone can reach a high accuracy (>90%) [29, 30]. The primary differential diagnosis of a low-grade clear-cell RCC is normal renal tubular cells (Fig. 13.2a) and adrenal cortical adenoma (Fig. 13.20), whereas that of a high-grade RCC includes adrenal cortical carcinoma (Fig. 13.21) and epithelioid angiomyolipoma.

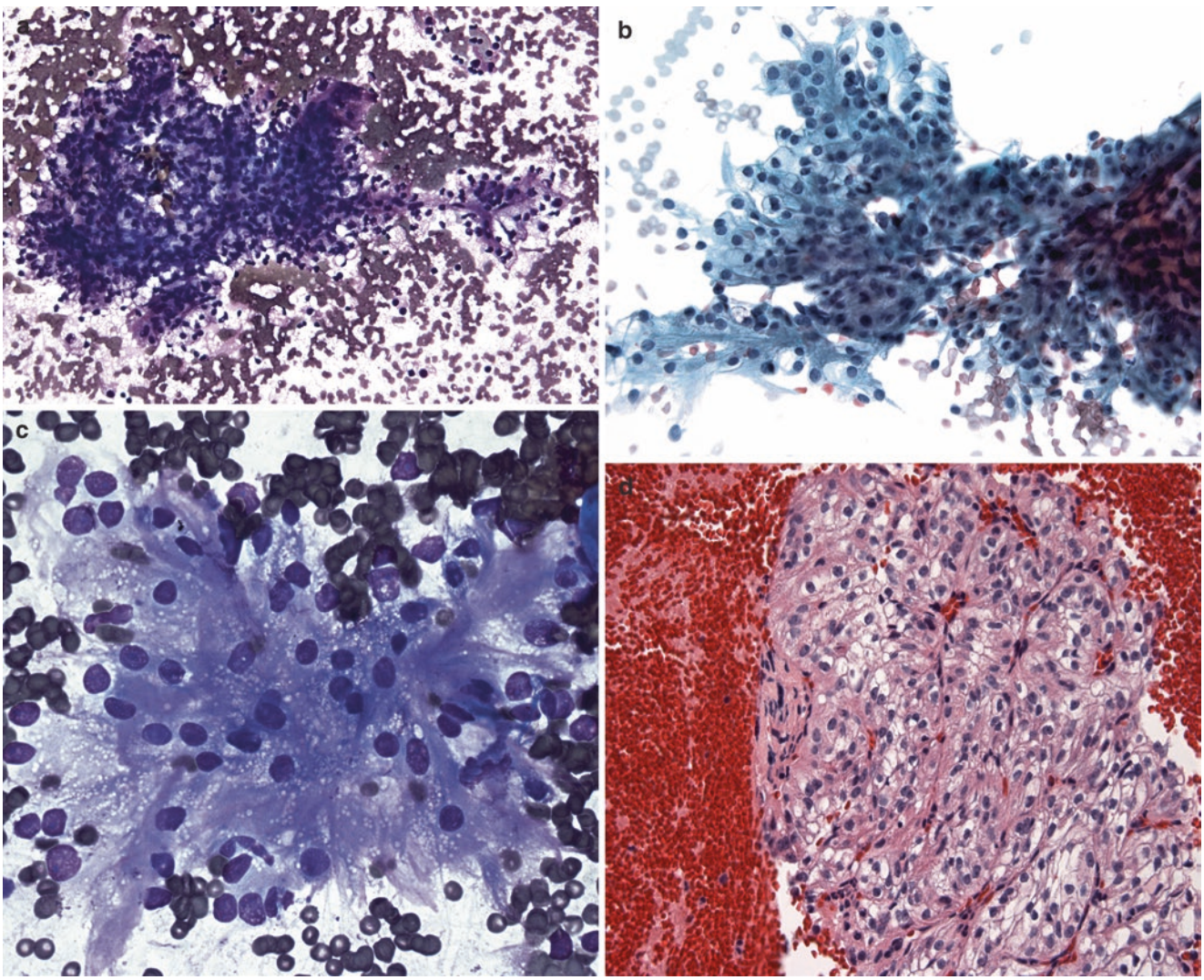

Fig. 13.9 Clear-cell renal cell carcinoma. (**a**, **b**) Tumor cells arranged in sheets or in clusters with transgressing thin capillaries (**a** DQ; **b** Pap stain). (**c**) Smaller clusters of tumor cells can be displayed like "butterfly." Tumor cells are characterized by low N/C ratios; round nuclei with prominent nucleoli; abundant, clear to granular cytoplasm with numerous small vacuoles; and ill-defined cell borders (DQ stain). (**d**) Tumor tissue fragments can sometimes be recovered in cell block sections in a bloody aspirate (H&E)

Ancillary studies:
- Clear-cell RCCs are positive for RCC, CD10, EMA, AMACR, and CA IX (box-like); and negative for CK7 and CD117.
- Cytogenetics: deletions on chromosome 3p, the site of the tumor-suppressor gene involved in von Hippel–Lindau disease.

Cytologic features:
- Moderately cellular, bloody smears, and cell blocks
- Cohesive cellular clusters with or without blood vessels
- Low N/C ratio large tumor cells with an eccentrically located, nucleolated, and round nucleus, vacuolated, pale cytoplasm, and ill-defined cell borders
- Occasional hyaline globules

Differential diagnosis and problems in diagnosis:
- Normal renal tubular cells
- Papillary RCC
- Clear-cell papillary RCC
- Aggregates of histiocytes/macrophages
- Inadvertently sampled hepatocytes or adrenal tissue
- Angiomyolipoma
- Adrenal cortical carcinoma

Papillary Renal Cell Carcinoma

Papillary renal cell carcinoma (papillary RCC) represents 10–15% of RCCs and is defined by the presence of papillary architecture in at least 50% of the tumor. Papillary RCCs can be multifocal and associated with renal papillary cortical adenomas (<=1.5 cm in size). Owing to its diverse morphology and overlapping features with other subtypes of RCCs, the rate of correct subclassification of papillary RCC is only approximately 50% [30].

The smears of papillary RCC are typically hypercellular with large complex papillary clusters and few single cells at scanning power (Fig. 13.10a). In type 1 papillary RCCs, the tumor cells lining the fibrovascular stalks are small, cuboidal, and uniform and have bland, sometimes gloved, nuclei and scant cytoplasm (Fig. 13.10b), whereas in type II papillary RCCs, the tumor cells are large and have abundant granular cytoplasm and pleomorphic, nucleolated nuclei (Fig. 13.10c). The foamy macrophages, within the fibrovascular cores and/or singly dispersed, intracytoplasmic hemosiderin deposition, and large spheres of tumor cells are additional characteristic features for papillary RCC (Fig. 13.10d, e). Some morphologic variations, such as with clear-cell features (Fig. 13.10f) and focal mucin production (Fig. 13.10g), pose diagnostic challenges for subclassification. In such cases, immunohistochemical studies with a panel of CK7, AMACR, and CD10 markers and/or fluorescence in situ hybridization (FISH) studies would be helpful (Table 13.1).

Ancillary studies:
- Papillary RCCs are positive for CK7, AMACR, and CD10 and negative for RCC and CD117.
- Cytogenetics: trisomy of chromosomes 7, 16, and 17 and loss of chromosome Y.

Cytologic features:
- Hypercellular smears
- Papillary clusters of tumor cells with arborizing vessels
- Foamy macrophages
- Hemosiderin in tumor cells and/or in macrophages
- Two types of tumor cells:
  - Type 1 papillary RCC: uniformly small, cuboidal cells with bland gloved nuclei and scant cytoplasm
  - Type 2 papillary RCC: large, pleomorphic cells with round, nucleolated nuclei and abundant eosinophilic cytoplasm

Differential diagnosis and problems in diagnosis:
- Urothelial carcinoma vs. type 2 papillary RCC
- Metanephric adenoma vs. type 1 papillary RCC
- Papillary hyperplasia in cysts associated with dialysis or in polycystic kidney disease
- Conventional/clear-cell RCC
- Mucinous tubular and spindle cell carcinoma
- Translocation RCC
- Clear-cell papillary RCC

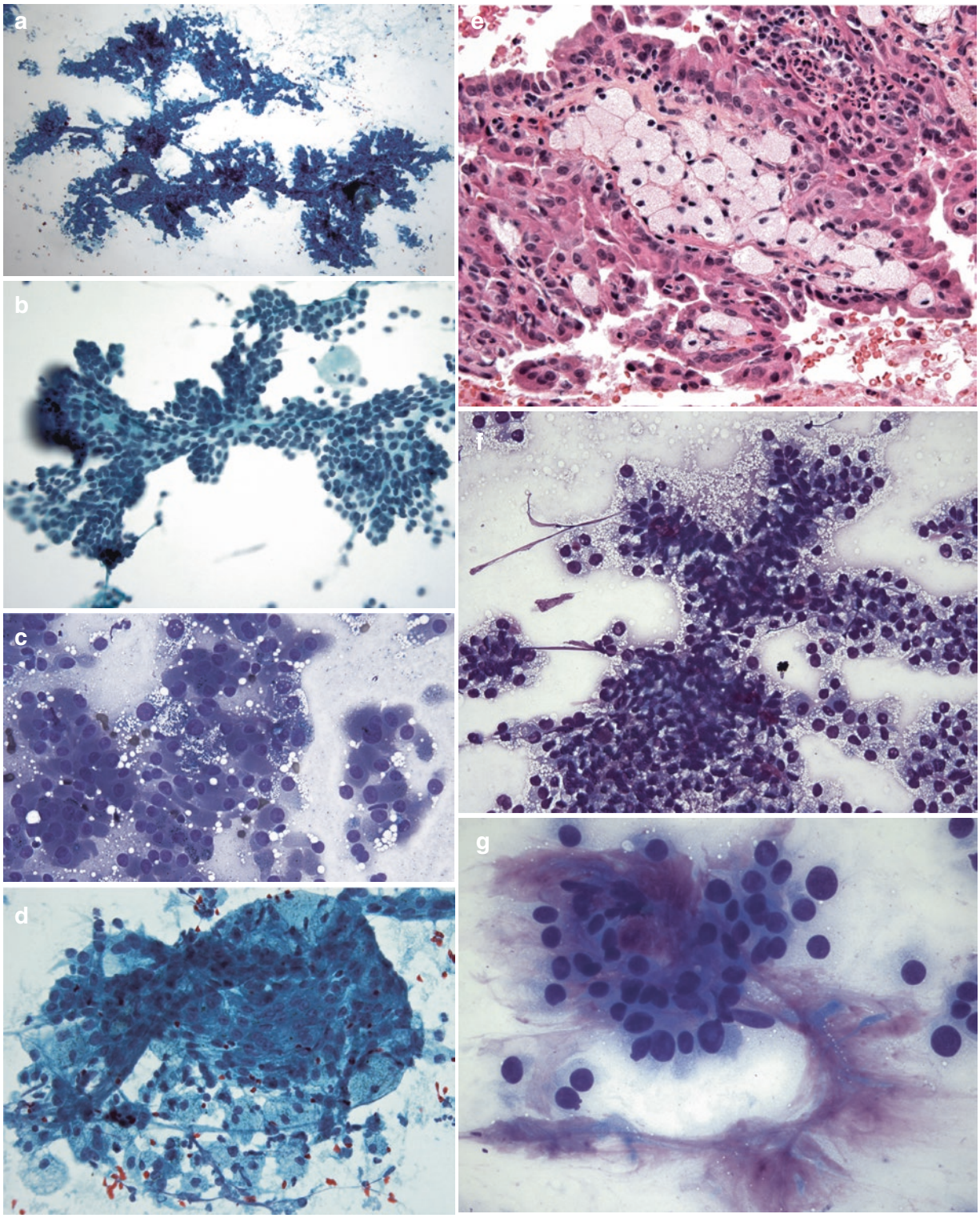

Fig. 13.10 Papillary renal cell carcinoma. (**a**) Scanning power shows a hypercellular aspirate with arborizing papillary structures (Pap stain). The tumor cells lining the fibrovascular stalks are small, cuboidal, and uniform in the type 1 papillary RCC (**b** Pap stain) or large, pleomorphic with abundant granular cytoplasm in the type II papillary RCC (**c** DQ stain). The foamy macrophages, hemosiderin pigments in macrophages and/or tumor cells (**c** DQ stain), and spherical clusters are additional characteristic features (**d** Pap stain). (**e**) Characteristic fibrovascular cores expanded by foamy macrophages are better appreciated in cell block sections (H&E). (**f**) Papillary RCC with clear-cell features evokes the differential diagnosis of translocation RCCs and clear-cell tubulopapillary RCC. (**g**) Focal mucin production brings mucinous tubular and spindle cell carcinoma in the differential diagnosis (DQ stain)

Chromophobe Renal Cell Carcinoma

Chromophobe renal cell carcinoma accounts for approximately 5% of all RCCs. It usually has a better prognosis than conventional or papillary RCC unless presenting at a higher TMN stage and/or with a sarcomatoid differentiation [31]. Therefore, recognizing chromophobe RCCs is of clinical importance, as a partial nephrectomy might be the treatment of choice for some patients.

Aspirates are at least moderately cellular and contain both dispersed and small clusters of tumor cells. Two principle types of tumor cells are intermingled: the large, polygonal cells with abundant, pale fluffy cytoplasm and the smaller granular cells with higher N/C ratios and more granular cytoplasm (Fig. 13.11a, d). The nuclei are centrally placed, hyperchromatic, and with an irregular, often winkled nuclear membrane. Binucleation is common. Pseudonuclear inclusions are occasionally seen (Fig. 13.11b, d). Two distinctive features of chromophobe RCC are the rigid, often thickened cell membrane and the perinuclear halo, giving a "koilocyte" appearance (Fig. 13.11d). The blood vessels, though not prominent, are also present, usually loosely associated with tumor cells (Fig. 13.11c).

Should the distinctive features of chromophobe RCC be absent, it could be difficult, on cytologic grounds alone, to separate it from oncocytoma or conventional RCC, especially the eosinophilic variant. Ancillary studies such as Hale's iron stain, immunohistochemistry, and cytogenetics could be helpful (see Table 13.1). Hale's iron stain shows diffuse cytoplasmic staining in chromophobe RCC (Fig. 13.11e), in contrast to focal apical staining in oncocytoma (Fig. 13.5d), and negative in conventional RCC. Because chromophobe RCC and oncocytoma are closely related, they share a similar immunoprofile. In addition, hybrid oncocytic/chromophobe tumors exist [32, 33]. Thus, distinguishing between the two is, sometimes, impossible. In such a scenario, a diagnosis of "oncocytic neoplasm" is warranted.

Ancillary studies:

- Chromophobe RCCs are positive for CK7 and AMACR and negative for RCC and CD117.
- Cytogenetics: monosomies for chromosomes 1, 2, 3, 6, 10, 13, 17, and 21.

Cytologic features:

- Moderately cellular smears with mainly single cells with well-defined cell borders
- Two types of cells: large, polygonal cells with abundant, pale fluffy cytoplasm and smaller granular cells with higher N/C ratio and more granular cytoplasm
- Perinuclear halo—koilocyte-like
- Frequent binucleation
- Variation in nuclear size, hyperchromasia, and winkled nuclear membrane

Differential diagnosis and problems in diagnosis:
- Oncocytoma
- Conventional RCC, granular cell variant
- Type 2 papillary RCC
- Normal proximal tubular cells

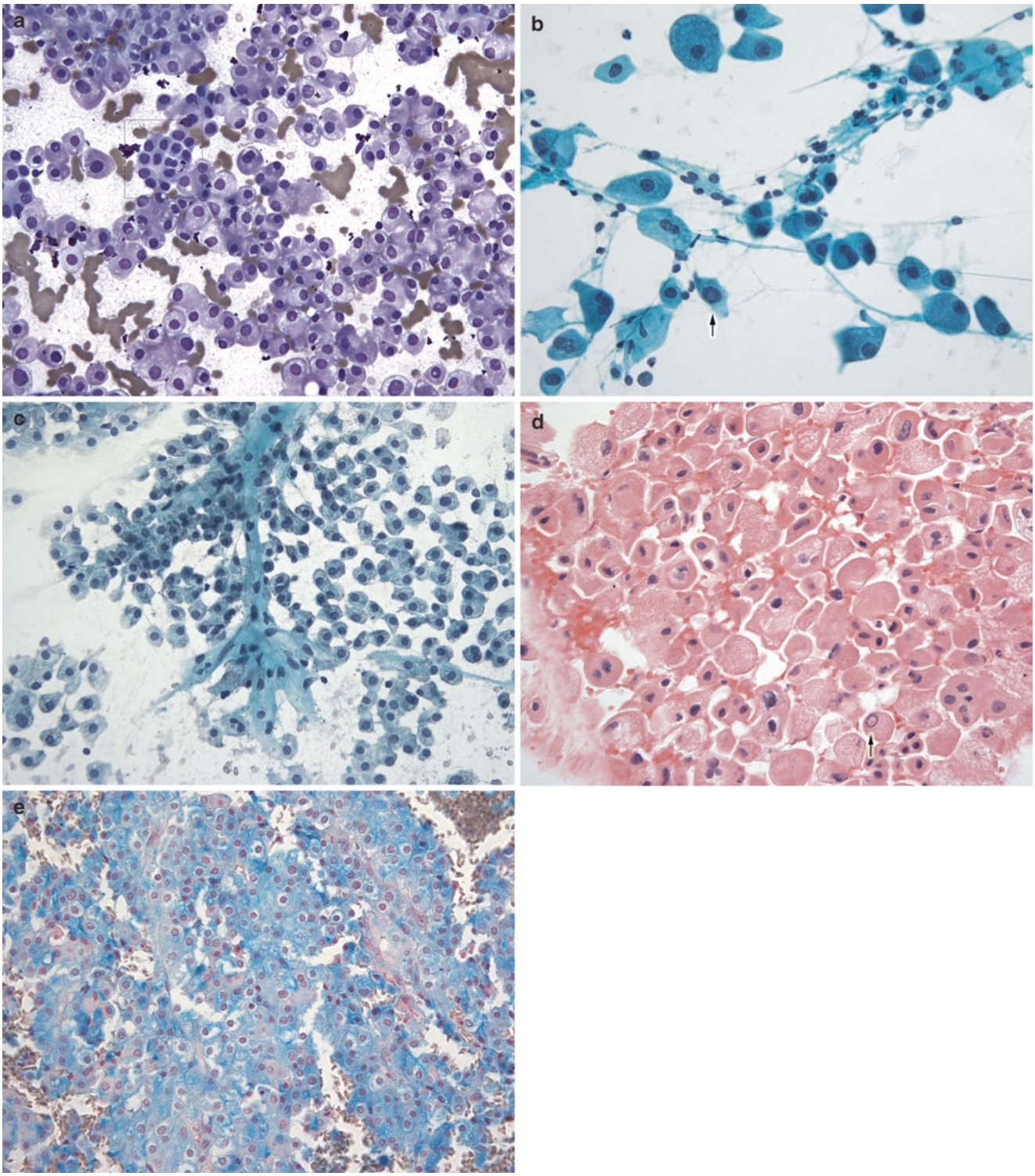

Fig. 13.11 Chromophobe renal cell carcinoma. Tumor cells, in variable sizes and distinctive cell borders, are mainly dispersed (**a** DQ stain; **b** Pap stain; **d** cell block H&E). Sometimes, tumor cells are loosely associated with vascular structures (**c** Pap stain). Two principle types of tumor cells: large, polygonal cells with abundant, pale fluffy cytoplasm (koilocyte-like) and smaller granular cells with a higher N/C ratio and more granular cytoplasm (**a** *in square*; **d** intermingled). Binucleation, winkled nuclear membrane, and intracytoplasmic pseudonuclear inclusions (*arrows*) are characteristic features (**b**, **d**). (**e**) A Hale's iron stain shows a diffuse cytoplasmic staining pattern

Sarcomatoid Renal Cell Carcinoma

Sarcomatoid RCC is not a distinct subtype of RCC but, rather, represents a common higher-grade transformation of different subtypes of RCC, mostly the clear-cell RCC. The diagnosis is relatively straightforward when both conventional RCC and the sarcomatoid component are present. Since the sarcomatoid transformation is often present only focally, an FNA sample could be underrepresentative. Once sampled, the sarcomatoid component yields cellular smears containing pleomorphic, spindled, and epithelioid cells in a necrotic background (Fig. 13.12a, b). In the absence of a usual RCC component, demonstrating the tumor cells with a renal epithelial differentiation (EMA+ and PAX-8+) is essential for establishing the diagnosis (Fig. 13.12c).

Differential diagnosis of sarcomatoid RCC:

- High-grade urothelial carcinoma
- Malignant PEComa
- Dedifferentiated liposarcoma

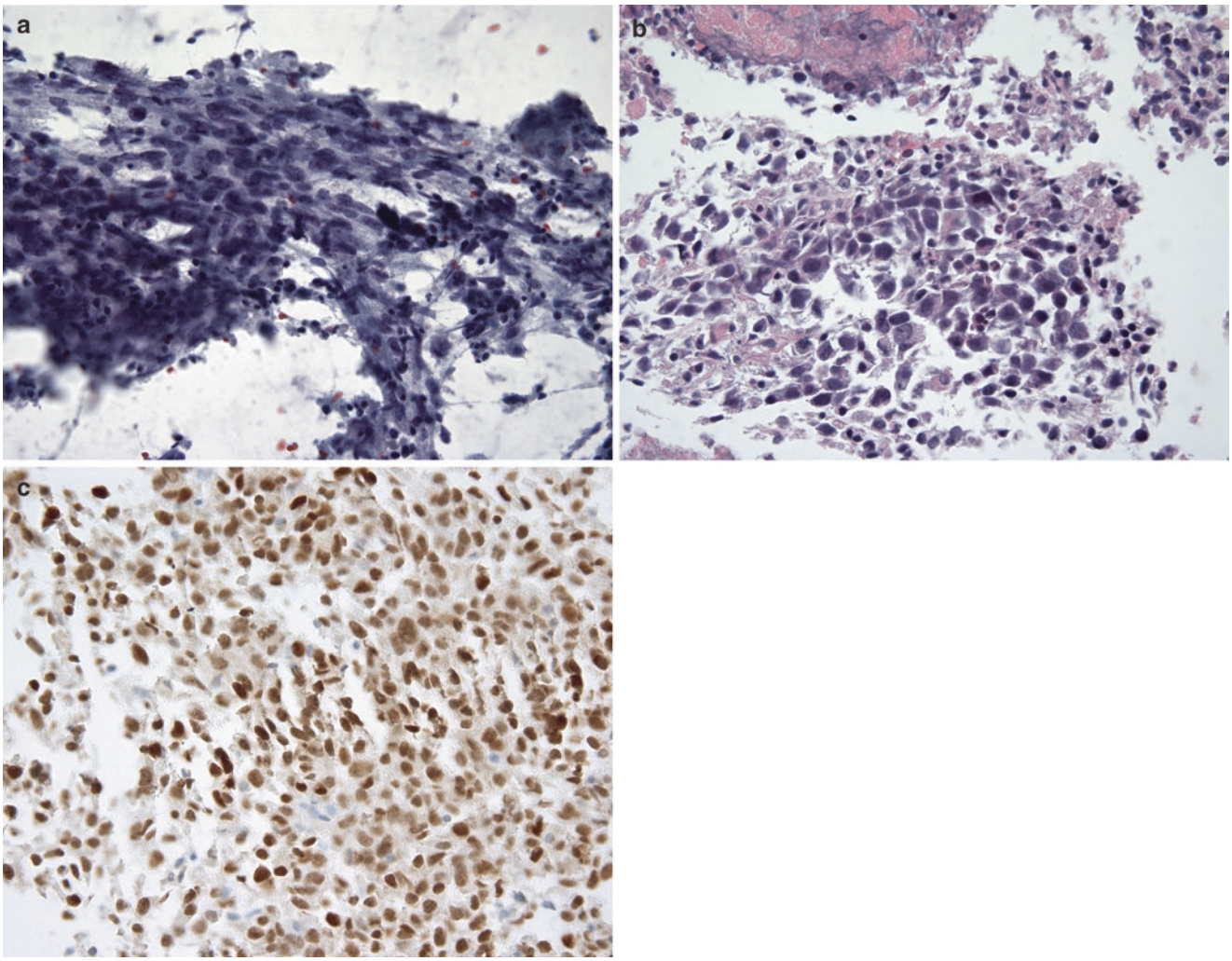

Fig. 13.12 Sarcomatoid renal cell carcinoma. Cellular smears with pleomorphic, spindled, and epithelioid cells in a necrotic background (**a** Pap stain; **b** cell block H&E). (**c**) Demonstration of nuclear positivity for PAX-8 is helpful to separate sarcomatoid RCC from mimics such as malignant PEComa or dedifferentiated liposarcoma

Renal Translocation Carcinoma

Renal translocation carcinomas are uncommon tumors that occur primarily in children and young adults. Most translocation carcinomas involve the transcription factor E3 (TFE3) located on Xp11.2, with ASPL-TFES or PRCC-TFE3 fusions. Another rare group of translocation carcinomas involve transcription factor EB (TFEB) with t(6;11) (p21;q12). These tumors are generally large in size (mean, 6–7 to 20 cm) and have a high prevalence of extrarenal extension and lymph node/visceral metastasis at the time of diagnosis [22, 34].

Histologically, the translocation carcinomas are characterized by a papillary and/or alveolar architecture, a mixture of clear and eosinophilic granular cells with voluminous cytoplasm and prominent nucleoli, and frequent calcifications. There are only rare case reports describing the cytologic findings of the translocation RCCs [35, 36]. The FNA smears are cellular with clusters ranging from papillae/spheres in variable sizes to large papillary structures, occasionally with a nested/alveolar pattern (Fig. 13.13a, b). The tumor cells have abundant clear to granular cytoplasm, well-defined cell borders, and prominent nucleoli (Fig. 13.13c). Hyaline nodules and psammoma bodies are frequent findings, which are clues to the diagnosis (Fig. 13.13d) [35, 37]. A strong clinical suspicion (young patient), demonstration of nuclear transcription factor (TFE3, TFEB) by immunohistochemistry, and/or identification of the translocation by molecular genetic tests (FISH, polymerase chain reaction [PCR]) are necessary to separate these tumors from clear-cell or other subtypes of RCC.

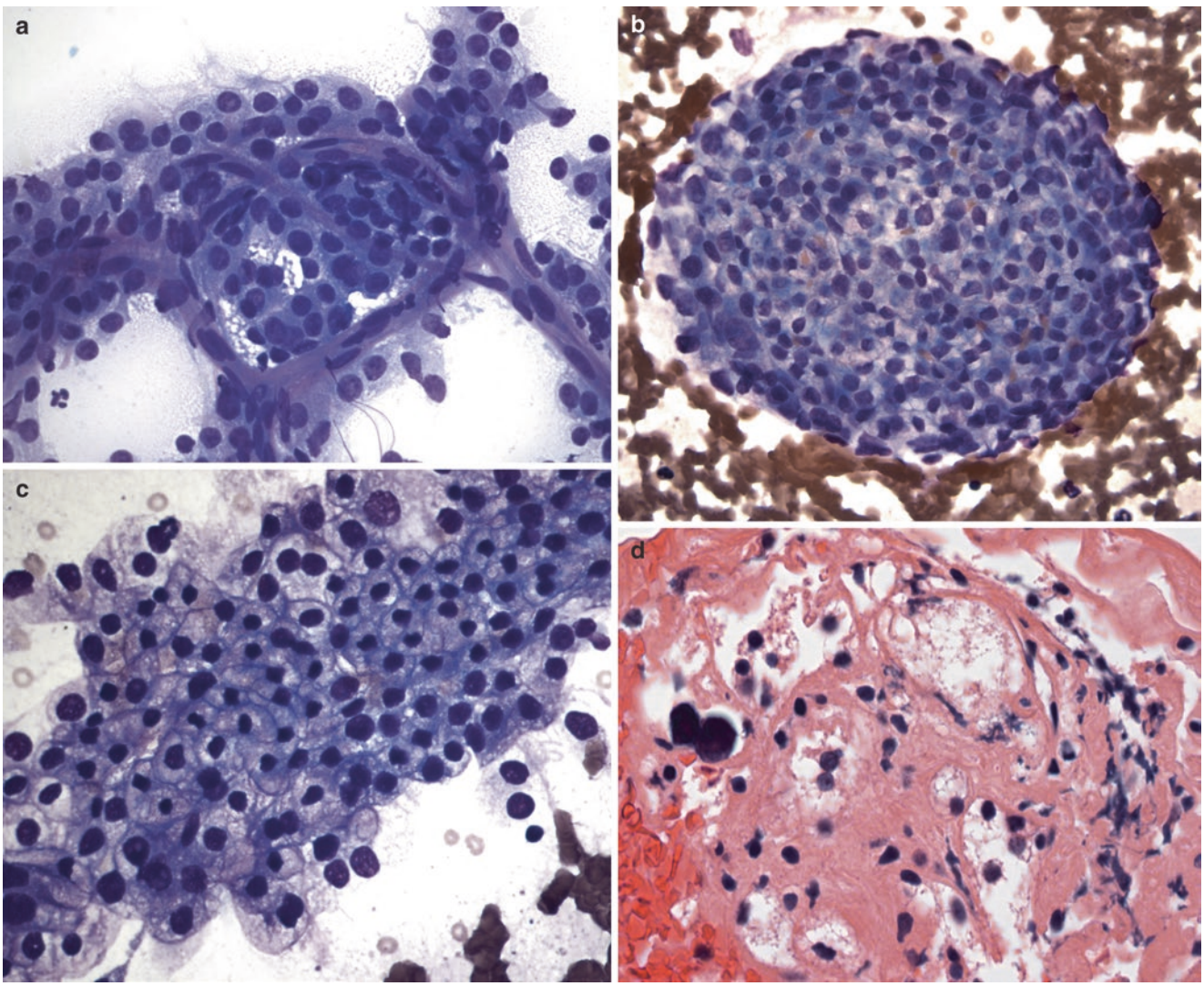

Fig. 13.13 Renal translocation carcinoma. Cellular arrangements include large papillary structures, occasionally with an alveolar pattern (**a**) and papillae/spheres (**b**) (DQ stain). (**c**) Tumor cells have abundant clear to granular cytoplasm, well-defined cell borders, and prominent nucleoli (DQ stain). (**d**) Frequent dense hyaline cores and/or psammoma bodies are clues to the diagnosis (cell block H&E)

Ancillary studies:

- Translocation carcinomas typically express CD10, RCC, and AMACR and infrequently express EMA and CK7. Specifically, the Xp11.2 translocation carcinoma shows nuclear staining for TFE3, whereas the TFEB translocation carcinoma shows nuclear staining for TFEB.
- Cytogenetics: Xp11.2 translocation with TFE3 fusions: *t*(X;1)(p11.2;q21) or *t*(X;17)(p11.2;q25) TFEB function: *t*(6;11)(p21;q12).

Cytologic features:

- Cellular smears with mainly clusters of tumor cells in papillae, alveolar, and/or papillary arrangements
- Tumor cells with well-defined borders, abundant clear to granular cytoplasm, slightly irregular nuclei, and prominent nucleoli
- Hyaline stroma and psammoma bodies

Differential diagnosis and problems in diagnosis:

- Conventional RCC
- Papillary RCC with clear-cell features
- Clear-cell papillary RCC

Mucinous Tubular and Spindle Cell Carcinoma

Mucinous tubular and spindle cell carcinoma (MTSCC) is a rare, low-grade renal epithelial neoplasm. It was recognized as a distinct entity by the World Health Organization 2004 Classification [38]. MTSCC has distinctive histomorphologic features, characterized by elongated tubules lined by cuboidal cells and/or cords of spindled cells set in a mucinous stroma. It occurs more commonly in women, with a wide age range. MTSCC usually has a more favorable prognosis than other types of RCCs [22, 39, 40].

The cytologic features of MTSCC have been reported in a few case reports [41–44]. Smears are cellular with isolated single cells and cellular clusters, many arranged in sheets, branching clusters, or pseudopapillary aggregates. The pseudopapillary aggregates contain capillary endothelial cells and basement membrane-like stroma but no true fibrovascular cores. The tumor cells, embedded in a metachromatic, vacuolated mucinous/myxoid stroma, are relatively bland and have ovoid to elongated nuclei, indistinct cell borders, and wispy to microvacuolated cytoplasm (Fig. 13.14a, b).

Ancillary studies:

- MTSCC expresses markers of proximal tubules (AMACR) and distal tubules (CK7) similar to papillary RCC. In addition, MTSCC infrequently expresses CD10, which is, in contrast, more frequently expressed in other types of RCC.
- Cytogenetics: loss of multiple chromosomes (see Table 13.1).

Cytologic features:

- Moderately cellular smears with both single cells and cellular clusters.
- Pseudopapillary aggregates contain capillary endothelial cells and basement membrane-like stroma.
- Bland tumor cells with oval to elongated nuclei, indistinct cell borders, and wispy cytoplasm.
- Mucinous/myxoid stroma.

Differential diagnosis and problems in diagnosis:

- Papillary RCC
- Conventional RCC
- Sarcomatoid RCC
- Low-grade smooth muscle tumor

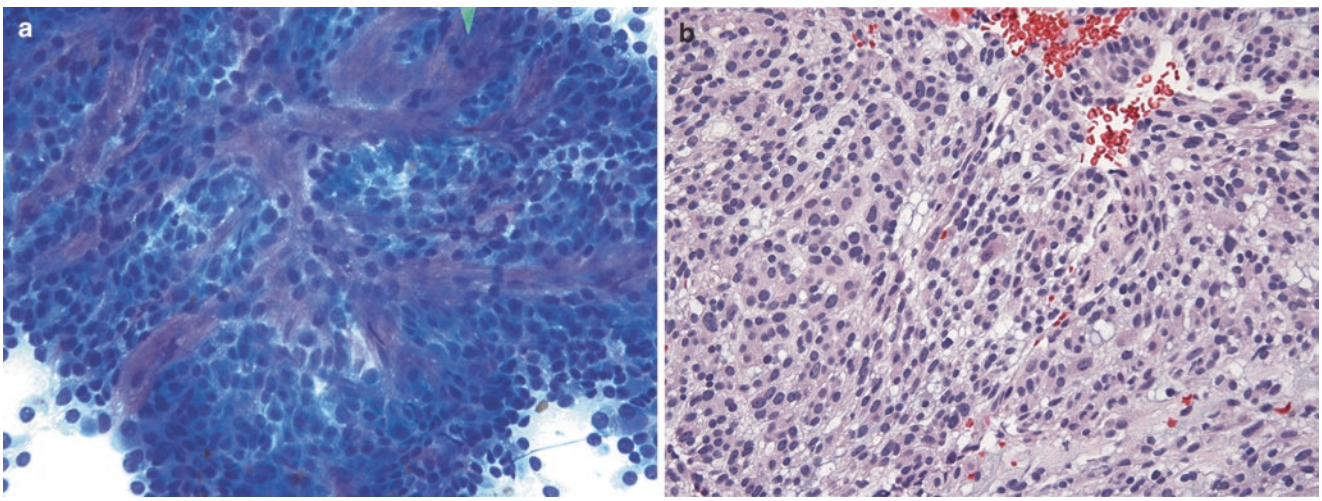

Fig. 13.14 Mucinous tubular and spindle cell carcinoma. (**a**) Pseudopapillary cellular clusters with basement membrane-like stroma and without true fibrovascular cores are typical. Dispersed tumor cells are cuboidal to plasmacytoid in shape and have round to oval nuclei, small nucleoli, and pale cytoplasm (DQ stain; courtesy of Rosemary H. Tambouret, MD, Massachusetts General Hospital, Boston, MA, USA). (**b**) Characteristic bland neoplastic cells in sheets and tubular arrangements and embedded in an abundant mucinous/myxoid stroma are more apparent in cell block sections (H&E)

Collecting Duct Carcinoma

Collecting duct carcinoma (CDC; Bellini tumor) is a rare malignant neoplasm of mesonephric duct derivation. It accounts for less than 1% of renal malignancy. CDC resembles renal pelvic urothelial carcinoma clinically and radiologically, and urine cytology may be positive [45]. The cytology features have been described in a few case reports [46, 47]. The smears are variably cellular, with both dispersed tumor cells and small cellular clusters. The tumor cells are those of a high-grade carcinoma: large nuclei with coarse chromatin and prominent nucleoli (Fig. 13.15). Nonspecific cytologic features and the rarity of CDC make the preoperative recognition of CDC extremely difficult. A PAX-8-positive and p63-negative immunoprofile supports a renal tubular rather than a urothelial differentiation, therefore the diagnosis of CDC [48].

Cytologic features:

- Variably cellular smear with both dispersed cells and small clusters
- High-grade carcinoma cells with large nuclei, coarse chromatin, and prominent nucleoli

Differential diagnosis and problems in diagnosis:

- Urothelial carcinoma
- Papillary RCC, high grade
- Metastatic carcinoma, high grade

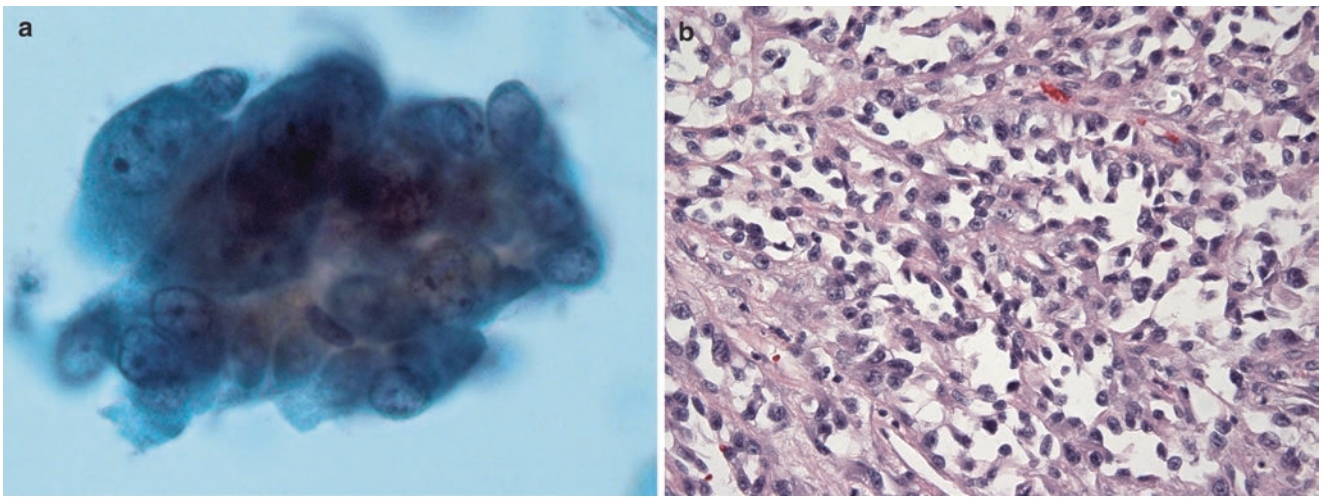

Fig. 13.15 Collecting duct carcinoma. (**a**) The tumors show nonspecific high-grade carcinoma features in a renal pelvic washing sample (SurePath, Pap stain). (**b**) Subsequent surgical resection shows tubulopapillary growth of high-grade, hobnail tumor cells (H&E)

Clear-Cell Papillary Renal Cell Carcinoma

Clear-cell papillary renal cell carcinoma (CCPRCC) is a newly recognized entity occurring in patients with or without end-stage kidney disease and is included in the WHO 2016 as a distinct subtype of RCC. It is the fourth most common subtype of RCC and is clinicopathologically distinct from both clear-cell RCC and pillillary RCC, which CCPRCC has likely been misdiagnosed as in the past. Characteristically, CCPRCC is composed of cuboidal or columnar cells with clear cytoplasm and low-grade nuclei in a picket-fence-like arrangement (Fig. 13.16a, b). It is important to recognize CCPRCC as it is associated with an indolent clinical course with an extremely low metastatic rate [49].

Ancillary studies:

- CCPRCC expresses CA IX in a characteristic cup-shaped staining pattern (Fig. 13.16d), which differs from the box-shaped staining pattern seen in clear-cell RCC. CCPRCC is also diffusely positive for CK7 (unlike CCRCC) (Fig. 13.16c) and negative for AMARC and CD10 (unlike PRCC). No specific chromosomal abnormalities have been identified.

Cytologic features:

- Nested, three-dimensional clusters
- Columnar cells or polygonal cells
- Clear cytoplasm with small vacuoles
- Low-grade, small, round to oval nuclei with fine-granular chromatin
- Nuclei located at one pole of the line of cells

Differential diagnosis and problems in diagnosis:

- Clear-cell RCC
- Papillary RCC
- Xp11.2 translocation RCC

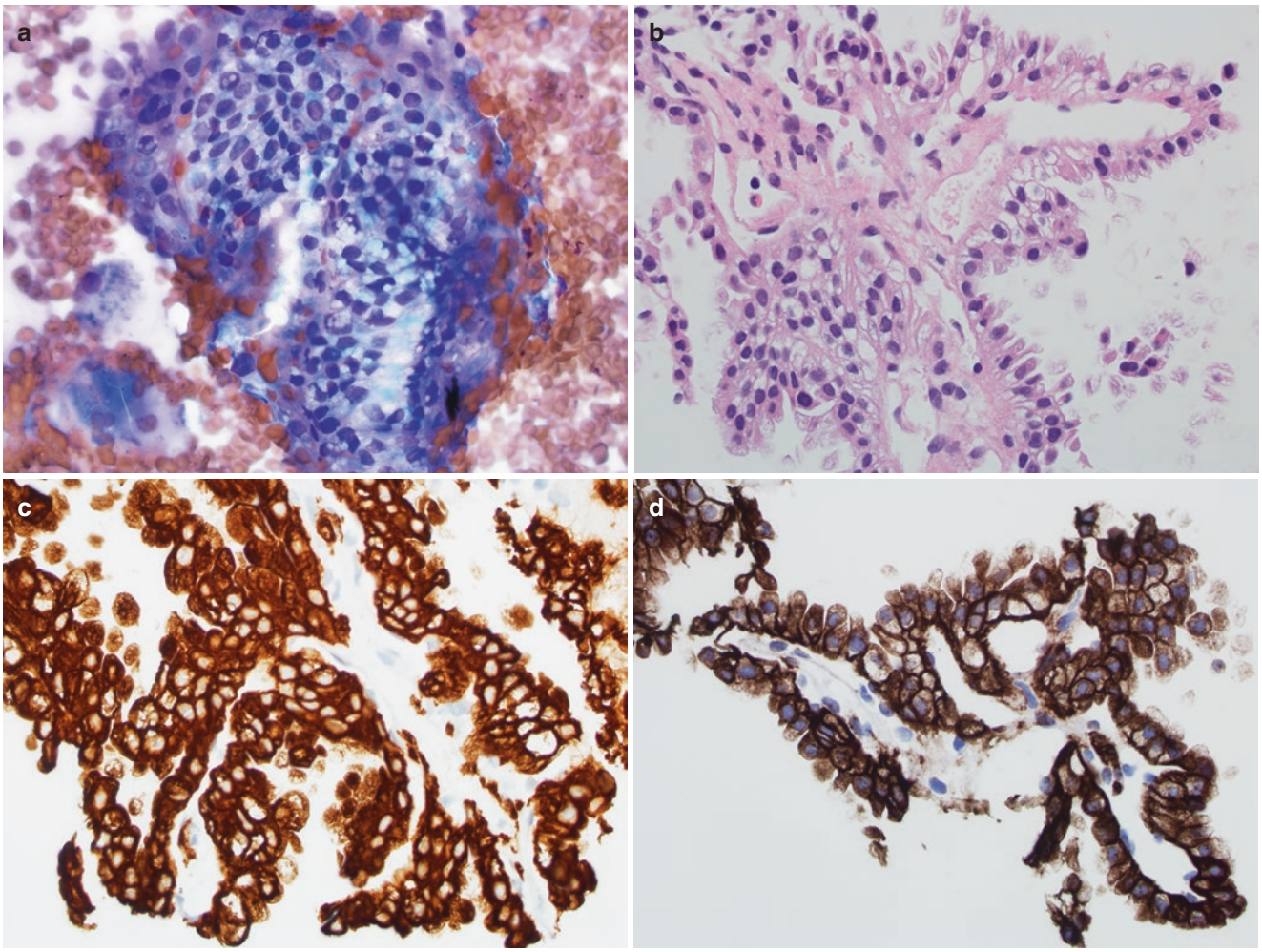

Fig. 13.16 Clear-cell papillary renal cell carcinoma (courtesy of Xiaoqi Lin, MD. PhD, Northwestern Memorial Hospital, Chicago, IL, USA). (**a**) Three-dimensional clusters of cuboidal tumor cells with eccentrically located, low-grade nuclei and clear, vacuolated cytoplasm (touch preparation of a core biopsy, Diff-Quik stain). (**b**) Core needle biopsy showing papillary/tubular architecture; columnar/cuboidal cells arranged in strips; small, round nuclei located away from the basement membrane (picket-fence-like arrangement); and clear cytoplasm (H&E). The presence of diffuse CK7 (**c**) and the characteristic cuplike staining pattern of CA IX (**d**) help distinguish it from clear-cell RCC

Urothelial Carcinoma

Urothelial carcinoma (UC) is a malignancy of the urothelium of the renal pelvis. It accounts for 5–10% of all renal tumors and 5% of all urothelial carcinomas. Similar to its bladder counterparts, UC occurs mainly in the elderly and multifocality is common. Most low-grade, noninvasive, papillary UCs are detected by upper urinary tract urine cytology and/or renal pelvic brushing, whereas the large, infiltrative, and high-grade tumors are likely sampled by FNA.

Owing to its central location and infiltrative nature, needle aspiration of an invasive UC is often technically challenging. Thus, the cellularity from aspiration varies. The aspirates are composed of small clusters and dispersed cells with scant to moderate amounts of dense cytoplasm and pleomorphic, hyperchromatic nuclei (Fig. 13.17a, b). The so-called cercariform cells with elongated cytoplasmic tails are usually a diagnostic clue to UC. Demonstrating reactivities for 34BE12, p63, and GATA3 by immunohistochemistry is helpful to distinguish UC from its mimics.

Cytologic features:

- Variably cellular smears
- Mainly dispersed cells in high-grade UC
- Cercariform cells with elongated, dense cytoplasm
- Hyperchromatic nuclei and irregular nuclear contours
- Necrosis and mitosis in high-grade UC

Differential diagnosis and problems in diagnosis:

- Sarcomatoid RCC
- Collecting duct carcinoma
- Metastatic carcinoma

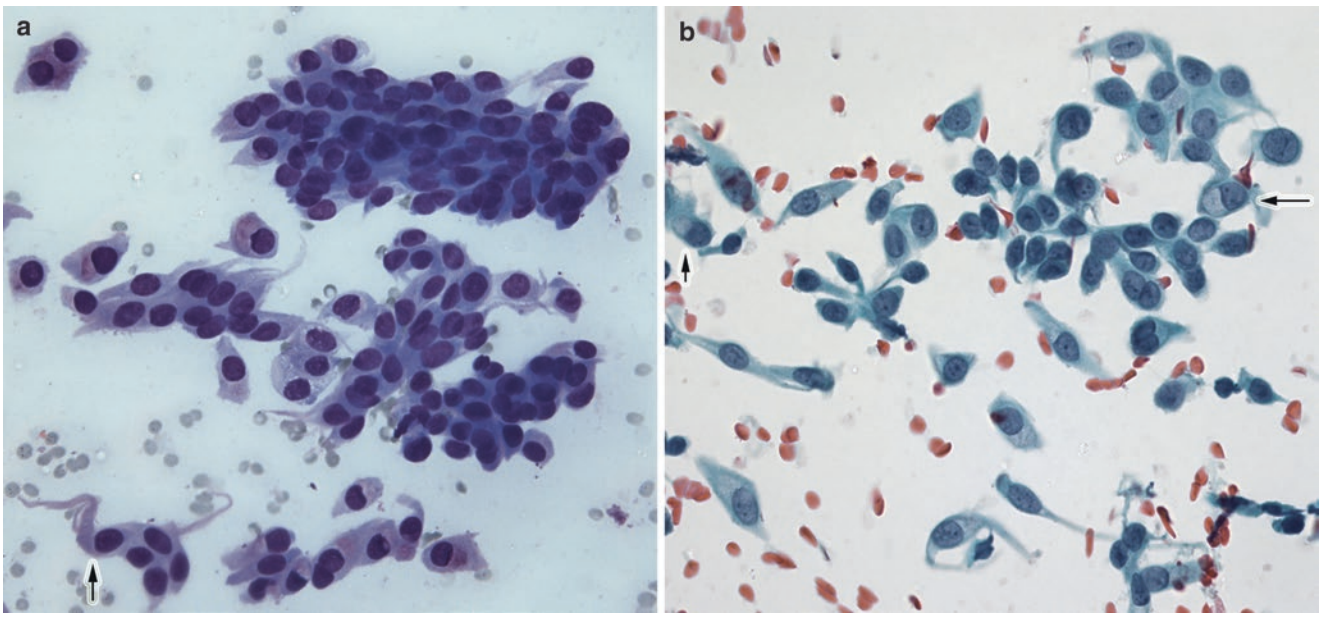

Fig. 13.17 Urothelial carcinoma. DQ-stained (**a**) and Pap-stained (**b**) smears showing clusters and dispersed tumor cells, many with an elongated cytoplasmic tail, resembling cercariform cells (**a** *arrow*). Glandular differentiation with intracellular mucin (**b** *arrows*) can also be seen in urothelial carcinoma

Lymphoma

The kidneys can be involved by Hodgkin or non-Hodgkin lymphomas, either in the context of widespread disease or as a primary presentation. Lymphoproliferative disorders count for approximately 3–5% of renal lesions evaluated by needle biopsies [50]. Diffuse large B-cell lymphoma is by far the most common form; rare entities, such as posttransplant lymphoproliferative disorder (PTLD) and intravascular lymphoma, are also encountered [51, 52].

Recognition of malignant lymphomas is extremely important as neither surgery nor cryoablation (the usual treatments for renal epithelial malignant neoplasms) is indicated. The details of diagnosing lymphomas are discussed in Chap. 8. It is worth mentioning that the presence of normal tubular cells in addition to the single lymphoid cells (easily missed!) can lead to a false impression of carcinoma.

Soft Tissue Tumors

Primary soft tissue tumors of the kidney are rare, except for angiomyolipoma. Malignant rhabdoid tumor (MRT) and synovial sarcoma are the most common sarcomas in children and in adults, respectively. Although rarely occurring in kidneys, epithelioid angiosarcoma, clear-cell sarcoma of the kidney, and PEComa pose significant diagnostic challenge as they can be easily mistaken for carcinoma due to their epithelioid morphology. Some sarcomas, such as dedifferentiated liposarcomas, occurring in adjacent perirenal soft tissue, usually infiltrate renal parenchyma and are often mistaken for a renal tumor. See Chap. (soft tissue) for more detailed discussion of these entities.

MRT is a rare, highly aggressive renal or extrarenal malignancy in infants. The aspirate smears are composed of large epithelioid cells in variable sizes, most with eccentrically located nuclei, open chromatin, prominent nucleoli, and abundant vacuolated cytoplasm, often with a dense intracytoplasmic (so-called rhabdoid) inclusion (Fig. 13.18). Cytogenetically, MRT is known to have mutations involving the *INI1* gene on chromosome 22q, which can be detected by immunohistochemistry and/or cytogenetic studies [53].

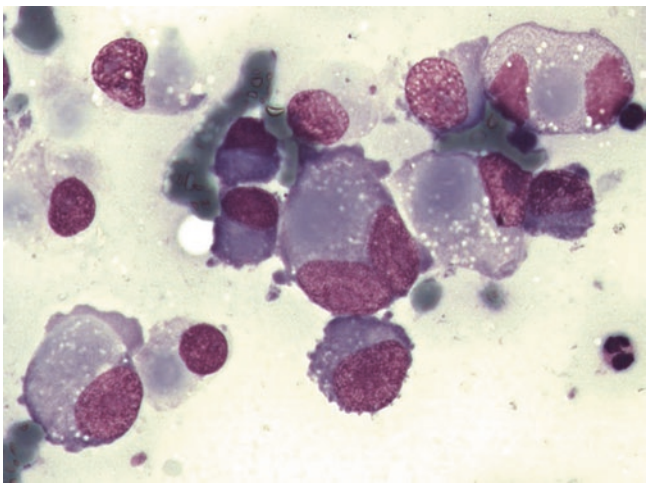

Fig. 13.18 Malignant rhabdoid tumor. The tumor cells are typically called "rhabdoid cells," which exhibit large epithelioid morphology, with eccentric nuclei, open chromatin, prominent nuclei, and characteristic dense cytoplasmic inclusions. Note the size of the tumor cells compared to that of the background inflammatory cells (DQ stain; courtesy of Jerzy Klijanienko, MD, Institut Curie, Paris, France)

The Adrenal Gland

Introduction

Adrenal masses are a common finding in abdominal image studies. Using CT, US, and more recently endoscopic US (EUS) guidance, FNA biopsy is effective in distinguishing primary, mostly benign adrenal nodules from metastatic tumors during staging workups [54–56]. It can also be used in establishing the diagnosis of some systemic infectious diseases such as disseminated histoplasmosis presenting as bilateral adrenal enlargement [57]. The accuracy of adrenal FNA is excellent with a sensitivity of at least 81% and a specificity approaching 100% [58–61]. On-site adequacy evaluation reduces sampling errors and improves overall accuracy [5]. The diagnostic pitfalls include misinterpretation of adrenal cortical tissue as renal clear-cell carcinoma or hepatocellular carcinoma; adrenal medulla as pheochromocytoma, or vice versa; and inability to distinguish adrenal cortical carcinoma from adenoma. Complications are rare and include hemorrhage, pneumothorax, needle tract seeding of tumor cells, and hypertensive crisis due to punctuation of pheochromocytoma [62–64].

Myelolipoma

Myelolipoma is a rare benign neoplasm of the adrenal gland or, more rarely, of the retroperitoneum and various other sites. It is composed of maturing hematopoietic elements and mature adipose tissue. It occurs unilaterally in older adults and presents variably from a small incidentaloma to a symptomatic massive tumor (>30 cm) with hemorrhage.

Aspirates show a mixture of normal fibroadipose tissue and bone marrow elements, in variable proportions (Fig. 13.19a, b). The identification of megakaryocytes is usually the most crucial step leading to the correct diagnosis.

Cytologic features:
- A mixture of mature fat and maturing hematopoietic elements
- Noticeable megakaryocytes

Differential diagnosis and problems in diagnosis:
- Angiomyolipoma
- Lipomatous tumor
- Extramedullary hematopoiesis

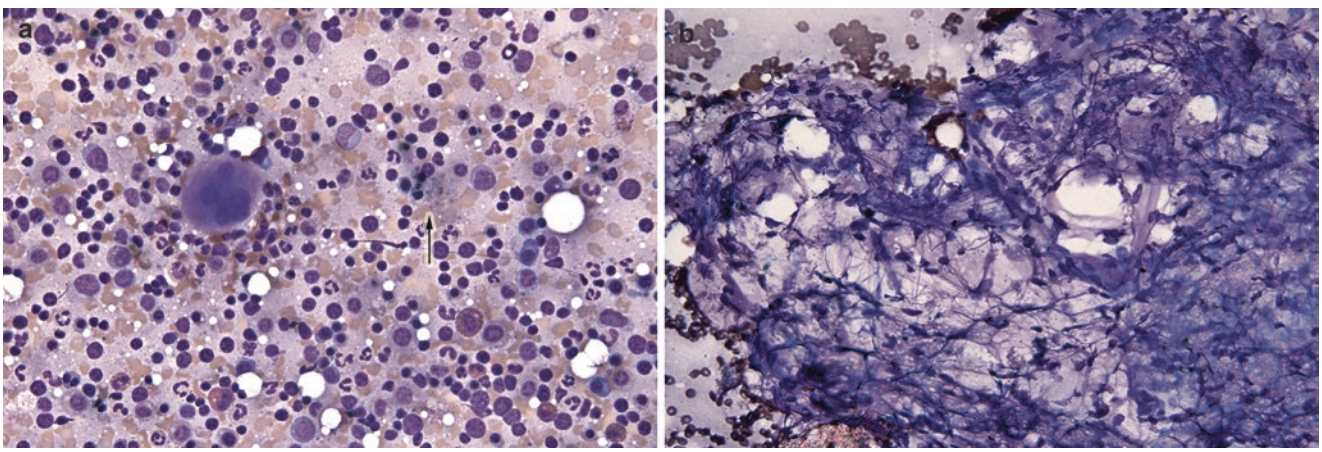

Fig. 13.19 Myelolipoma. (**a**) Cellular smear showing trilineage hematopoietic elements with a megakaryocyte in the center. Hemosiderin-laden macrophages (*arrow*) and calcifications are common in large lesions (DQ stain). (**b**) Adipose tissue, frequently admixed with hematopoietic elements and/or lymphocytes, gives a false impression of hypercellularity, mimicking liposarcoma (DQ stain)

Adrenal Cortical Neoplasm

Adrenal cortical adenomas occur in approximately 5% of adults and count for approximately 50% of all incidentaloma. As in other endocrine glands, true adenomas are unilateral and solitary, whereas hyperplastic adenomatous nodules can be bilateral and multinodular. The cytomorphology of normal cortex, hyperplastic nodule, and adenoma is indistinguishable; therefore, a diagnosis of benign adrenal cortical tissue, or nodules, or adenoma can only be rendered in conjunction with clinical and radiological correlation [65]. The typical smears are at least moderately cellular, with numerous naked, round, and uniform nuclei in a "frothy" microvesicular lipid or granular background (Fig. 13.20a, b). Large cellular clusters with wrapping endothelial cells or transgressing vessels are also present (Fig. 13.20c). The intact cells have either granular or vacuolated cytoplasm with indistinct cell borders (Fig. 13.20b). Random nuclear enlargement (endocrine atypia) can be seen, but mitoses or necrosis should be minimal.

Cytologic features:

- At least moderately cellular smears
- Microvesicular lipid background
- Numerous naked, round nuclei
- Intact cells with indistinct cell borders and granular or vacuolated cytoplasm
- Lack of necrosis and mitosis

Differential diagnosis and problems in diagnosis:

- Adrenal cortical carcinoma
- Renal clear-cell carcinoma
- Hepatocytes

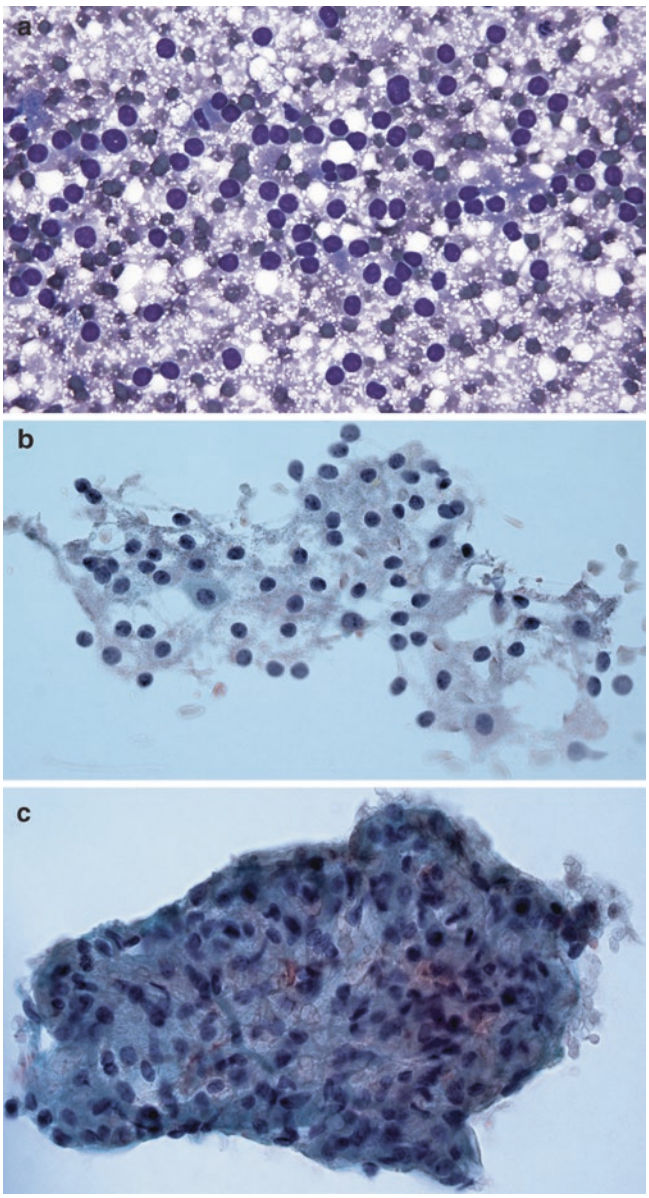

Fig. 13.20 Adrenal cortical nodule/adenoma. Cellular aspirate with numerous dispersed, relatively uniform bare nuclei in a frothy cytoplasmic background, indistinguishable from normal adrenal cortical tissue (**a**) DQ stain; (**b**) Pap stain). (**c**) Large cellular clusters with wrapping endothelial cells can also occur

Adrenal Cortical Carcinoma

Adrenal cortical carcinoma is a rare tumor with a bimodal age distribution peaking at younger than 6 years old and between the ages of 30 and 50 years. In contrast to adenomas, the tumor is usually large (>5–6 cm), unilateral, and functional (up to 80%). Cushing syndrome may be the first clinical presentation, and virilizing or feminizing adrenal tumors are likely to be malignant. Metastases are commonly present at diagnosis and help to prove malignancy.

The aspirate smears from most cases show obvious malignancy: hypercellular smears with predominantly intact single cells in a necrotic background. The tumor cells exhibit moderate to marked cytologic atypia with diffusely large, atypical nuclei, granular to vacuolated cytoplasm, and prominent nucleoli (Fig. 13.21a, b). An increased number of mitosis, especially atypical mitotic figures (Fig. 13.21c), are a clue to malignancy [66]. Because many histological criteria for malignancy, such as capsular and/or vascular invasion, cannot be evaluated on FNA samples, definitive distinction of a well-differentiated malignant tumor from an adrenal adenoma can be extremely difficult. Therefore, in equivocal cases, the interpretation "atypical adrenal cortical neoplasm" should be considered and surgical resection be advised. Cells of adrenal cortical origin express inhibin, Melan A, and calretinin by immunohistochemistry (Fig. 13.21d) and are negative for epithelial membrane antigen (EMA), which is helpful in distinguishing them from RCCs and hepatocytes, as well as in establishing the diagnosis at a metastatic site.

Cytologic features:

- Hypercellular smears with a necrotic background
- Usually dispersed intact cells with granular or vacuolated cytoplasm
- Eccentrically located nuclei with diffuse nuclear atypia
- Mitoses including atypical forms

Differential diagnosis and problems in diagnosis:

- Adrenal adenoma
- Renal cell carcinoma
- Pheochromocytoma
- Metastatic, poorly differentiated, large-cell carcinoma
- Metastatic melanoma
- High-grade pleomorphic sarcoma

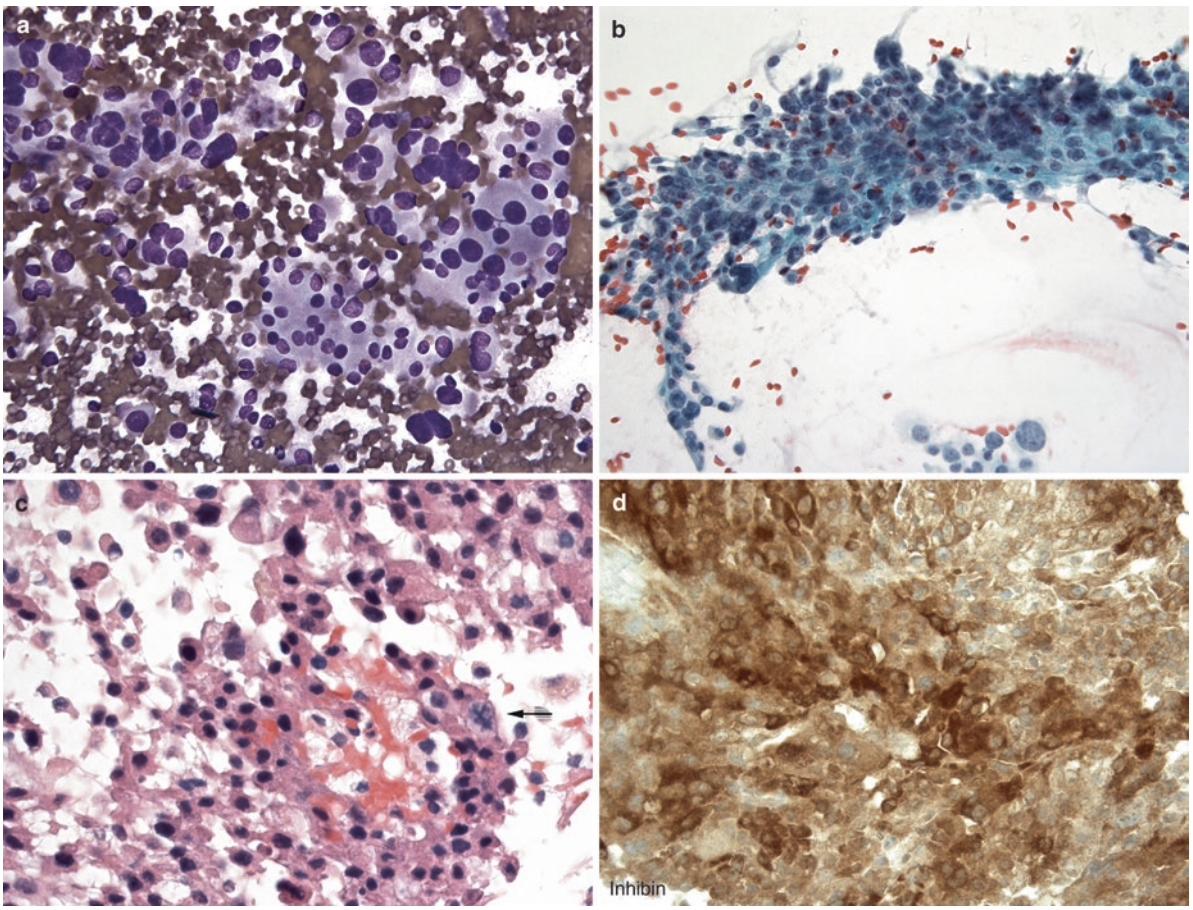

Fig. 13.21 Adrenal cortical carcinoma. The tumor cells usually exhibit diffuse and marked cytologic atypia and pleomorphism (**a** DQ stain; **b** Pap stain). (**c**) Necrosis and mitoses, especially atypical ones (*arrow*), are clues to malignancy (cell block, H&E). (**d**) Demonstration of immunoreactivity for inhibin and/or Melan A is helpful to separate adrenal cortical carcinoma from its mimics such as RCC

Pheochromocytoma

Pheochromocytoma is the primary tumor of the adrenal medulla and usually causes paroxysmal hypertension, palpitation, and even cardiac arrhythmia due to the release of excessive catecholamines by the tumor cells. Approximately 10–20% of the cases are associated with familial neoplastic syndromes, such as the MEN 2a and 2b, NF1, and the VHL syndrome. The same tumor can also occur in the extra-adrenal site, commonly in retroperitoneum, and it is called paraganglioma [67]. The majority of patients are diagnosed based on hypertension, the elevated blood and urinary levels of catecholamines and their metabolites, and an adrenal or paraspinal mass. Therefore, a preoperative biopsy such as FNA is usually unnecessary. Although FNA is not necessarily a contraindication, any aspiration of a possible pheochromocytoma/paraganglioma should be performed in a clinic staffed with clinicians and equipped with tools that are essential to control a potential hypertensive crisis [63].

FNAs of pheochromocytoma or paraganglioma usually yield cellular smears with a bloody background, like those of many other hypervascular endocrine organs. The smears are composed of predominantly dispersed single cells and small clusters (Fig. 13.22a). Cellular clusters containing vessels can also occur. The tumor cells exhibit neuroendocrine cytomorphology: polygonal to plasmacytoid in shape, ground nuclei with salt/pepper chromatin, and cytoplasmic granules on Romanowsky-based stains (Fig. 13.22b). Marked nuclear pleomorphism/anaplasia and scattered spindled cells are common (Fig. 13.22c, d), but necrosis and mitoses are unusual findings. The classic Zellballen pattern can be appreciated in cell block or core biopsy material (Fig. 13.22e). Demonstration of neuroendocrine differentiation by immunostains for chromogranin and synaptophysin and a lack of cytokeratin expression differentiate them from adrenal cortical carcinomas and other neuroendocrine carcinomas.

Cytologic features:
- Cellular smears in a bloody background
- Dispersed epithelioid/plasmacytoid cells and spindled cells
- Salt/pepper chromatin, ill-defined cytoplasm, and red cytoplasmic granules
- Bare nuclei, binucleation, and nuclear pleomorphism

Differential diagnosis and problems in diagnosis:
- Adrenal cortical carcinoma
- Metastatic neuroendocrine carcinoma
- Metastatic sarcoma or melanoma with a mixed spindle and epithelioid pattern

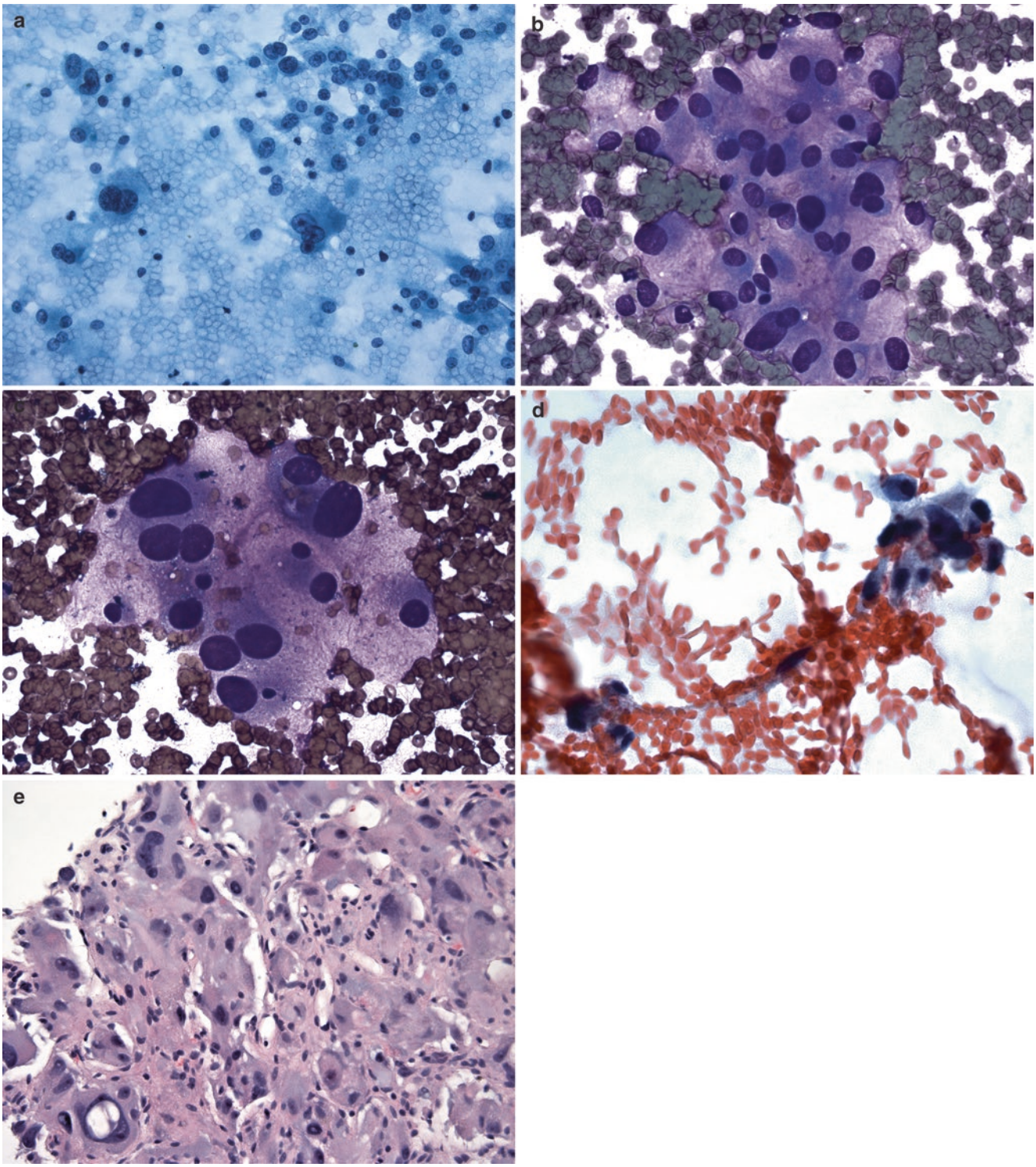

Fig. 13.22 Pheochromocytoma. (**a**) Cellular bloody smears with dispersed single cells, some in small clusters. Bare nuclei and binucleation are common (Pap stain). (**b**) Tumor cells have round to oval nuclei with salt/pepper chromatin and cytoplasmic granules (DQ stain). Marked pleomorphism (**c** DQ stain) and spindled cells (**d** Pap stain) can be mistaken for malignancy. (**e**) Core histologic section showing the typical Zellballen pattern, which is absent from most smear preparations (H&E)

Metastasis

FNA is generally the approach of choice to confirm or rule out a metastasis in a patient with a history of malignancy and to establish a tissue diagnosis in a patient presented with a widely metastatic disease of unknown primary. Metastatic diseases count for more than 70–80% of all adrenal FNAs with a neoplastic diagnosis [68]. The most common sites of origin include lung (both small cell carcinoma and adenocarcinoma), melanoma, and RCC [69, 70]. See respective chapters for detailed cytomorphology of metastatic lung carcinoma (see Figs. 7.13, 7.14, 7.15, 7.16, 7.17, 7.18, 7.19, 7.20, and 7.21), renal cell carcinoma (see Figs. 13.9, 13.10, 13.11, 13.12, and 13.13), and melanoma (see Figs. 9.82, 15.25, and 15.26).

Differential diagnosis of metastases:

- Metastatic RCC vs. adrenal cortical neoplasm
- Metastatic small cell carcinoma vs. bare nuclei of adrenal cortical cells
- Metastatic neuroendocrine carcinoma vs. pheochromocytoma
- Metastatic prostatic adenocarcinoma vs. adrenal cortical neoplasm

References

1. Silverman SG, Gan YU, Mortele KJ, Tuncali K, Cibas ES. Renal masses in the adult patient: the role of percutaneous biopsy. Radiology. 2006;240:6–22.
2. Roh MH, Dal Cin P, Silverman SG, Cibas ES. The application of cytogenetics and fluorescence in situ hybridization to fine–needle aspiration in the diagnosis and subclassification of renal neoplasms. Cancer Cytopathol. 2010;118:137–45.
3. Phe V, Yates DR, Renard-Penna R, Cussenot O, Roupret M. Is there a contemporary role for percutaneous needle biopsy in the era of small renal masses? BJU Int. 2012;109:867–72.
4. Herrera GA, Turbat-Herrera EA. Ancillary diagnostic techniques in the evaluation of adult epithelial renal neoplasms: indications, caveats, and pitfalls. Appl Immunohistochem Mol Morphol AIMM Off Publ Soc Appl Immunohistochem. 2014;22(2):77–98.
5. Burlingame OO, Kesse KO, Silverman SG, Cibas ES. On-site adequacy evaluations performed by cytotechnologists: correlation with final interpretations of 5241 image-guided fine-needle aspiration biopsies. Cancer Cytopathol. 2012;120(3):177–84.
6. Yang CS, Choi E, Idrees MT, Chen S, Wu HH. Percutaneous biopsy of the renal mass: FNA or core needle biopsy? Cancer Cytopathol. 2017;125(6):407–15.
7. Truong LD, Shen SS. Immunohistochemical diagnosis of renal neoplasms. Arch Pathol Lab Med. 2011;135:92–109.
8. Schmitt F, Barroca H. Role of ancillary studies in fine–needle aspiration from selected tumors. Cancer Cytopathol. 2012;120:145–60.
9. Fulciniti F, Mascolo M, Insabato L, et al. Massive infarction of papillary carcinoma of the kidney after fine needle aspiration biopsy: report of a case with cytohistologic correlation. Acta Cytol. 2006;50:563–6.
10. Turbiner J, Amin MB, Humphrey PA, Srigley JR, De Leval L, Radhakrishnan A, et al. Cystic nephroma and mixed epithelial and stromal tumor of kidney: a detailed clinicopathologic analysis of 34 cases and proposal for renal epithelial and stromal tumor (REST) as a unifying term. Am J Surg Pathol. 2007;31:489–500.
11. Yusenko MV. Molecular pathology of renal oncocytoma: a review. Int J Urol. 2010;17:602–12.
12. Conner JR, Hirsch MS, Jo VY. HNF1beta and S100A1 are useful biomarkers for distinguishing renal oncocytoma and chromophobe renal cell carcinoma in FNA and core needle biopsies. Cancer Cytopathol. 2015;123(5):298–305.
13. Zhou H, Guo M, Gong Y. Challenge of FNA diagnosis of angiomyolipoma: a study of 33 cases. Cancer Cytopathol. 2017;125(4):257–66.
14. Khayyata S, Grignon DJ, Aulicino MR, Al-Abbadi MA. Metanephric adenoma vs. Wilms' tumor: a report of 2 cases with diagnosis by fine needle aspiration and cytologic comparisons. Acta Cytol. 2007;51:464–7.
15. Patel NP, Geisinger KR, Zagoria RJ, Bergman S. Fine needle aspiration biopsy of metanephric adenoma: a case report. Acta Cytol. 2009;53:327–31.
16. Olgac S, Hutchinson B, Tickoo SK, Reuter VE. Alpha–methylacyl–CoA racemase as a marker in the differential diagnosis of metanephric adenoma. Mod Pathol. 2006;19:218–24.
17. Charles AK, Mall S, Watson J, Berry PJ. Expression of the Wilms' tumour gene WT1 in the developing human and in paediatric renal tumours: an immunohistochemical study. Mol Pathol. 1997;50:138–44.
18. Sugie S, Tanaka T, Nishikawa A, Yoshimi N, Kato K, Mori H, et al. Fine–needle aspiration cytology of xanthogranulomatous pyelonephritis. Urology. 1991;37:376–9.
19. Li L, Parwani AV. Xanthogranulomatous pyelonephritis. Arch Pathol Lab Med. 2011;135:671–4.
20. Eble JN, Togashi K, Pisani P. Renal cell carcinoma. In: Eble JN, Sauter G, Epstein JI, Sesterhenn IA, editors. Pathology and genetics of tumors of the urinary system and male genital organs world health organization classification of tumors. Lyon: IARC Press; 2004. p. 12–4.
21. Lopez-Beltran A, Montironi R, Egevad L, Caballero-Vargas MT, Scarpelli M, Kirkali Z, et al. Genetic profiles in renal tumors. Int J Urol. 2010;17:6–19.
22. Srigley JR, Delahunt B. Uncommon and recently described renal carcinomas. Mod Pathol. 2009;22:S2–23.
23. Kovacs G, Akhtar M, Beckwith BJ, Bugert P, Cooper CS, Delahunt B, et al. The Heidelberg classification of renal cell tumours. J Pathol. 1997;183:131–3.
24. Storkel S, Eble JN, Adlakha K, Amin M, Blute ML, Bostwick DG, et al. Classification of renal cell carcinoma: workgroup no. 1. Union Internationale Contre le Cancer (UICC) and the American Joint Committee on Cancer (AJCC). Cancer. 1997;80:987–9.
25. Aydin H, Chen L, Cheng L, Vaziri S, He H, Ganapathi R, et al. Clear cell tubulopapillary renal cell carcinoma: a study of 36 distinctive low–grade epithelial tumors of the kidney. Am J Surg Pathol. 2010;34:1608–21.
26. Amin MB, MacLennan GT, Gupta R, Grignon D, Paraf F, Vieillefond A, et al. Tubulocystic carcinoma of the kidney: clinicopathologic analysis of 31 cases of a distinctive rare subtype of renal cell carcinoma. Am J Surg Pathol. 2009;33:384–92.
27. Moch H, Cubilla AL, Humphrey PA, Reuter VE, Ulbright TM. The 2016 WHO classification of tumours of the urinary system and male genital organs-part a: renal, penile, and testicular tumours. Eur Urol. 2016;70(1):93–105.
28. Bishop JA, Hosler GA, Kulesza P, Erozan YS, Ali SZ. Fine–needle aspiration of renal cell carcinoma: is accurate Fuhrman grading possible on cytologic material? Diagn Cytopathol. 2011;39:168–71.

29. Renshaw AA, Lee KR, Madge R, Granter SR. Accuracy of fine needle aspiration in distinguishing subtypes of renal cell carcinoma. Acta Cytol. 1997;41:987–94.
30. Adeniran AJ, Al-Ahmadie H, Iyengar P, Reuter VE, Lin O. Fine needle aspiration of renal cortical lesions in adults. Diagn Cytopathol. 2010;38:710–5.
31. Cheville JC, Lohse CM, Sukov WR, Thompson RH, Leibovich BC. Chromophobe renal cell carcinoma: the impact of tumor grade on outcome. Am J Surg Pathol. 2012;36:851–6.
32. Adley BP, Schafernak KT, Yeldandi AV, Yang XJ, Nayar R. Cytologic and histologic findings in multiple renal hybrid oncocytic tumors in a patient with Birt–Hogg–Dube syndrome: a case report. Acta Cytol. 2006;50:584–8.
33. Petersson F, Gatalica Z, Grossmann P, Perez Montiel MD, Alvarado Cabrero I, Bulimbasic S, et al. Sporadic hybrid oncocytic/chromophobe tumor of the kidney: a clinicopathologic, histomorphologic, immunohistochemical, ultrastructural, and molecular cytogenetic study of 14 cases. Virchows Arch. 2010;456:355–65.
34. Argani P, Ladanyi M. Renal carcinoma associated with Xp11.2 translocations/TFE3 fusions. In: Eble JN, Sauter G, Epstein JI, Sesterhenn IA, editors. Pathology and genetics of tumors of the urinary system and male genital organs world health organization classification of tumors. Lyon: IARC Press; 2004. p. 37–8.
35. Schinstine M, Filie AC, Torres-Cabala C, Abati A, Linehan WM, Merino M. Fine–needle aspiration of a Xp11.2 translocation/TFE3 fusion renal cell carcinoma metastatic to the lung: report of a case and review of the literature. Diagn Cytopathol. 2006;34:751–6.
36. Yamaguchi T, Kuroda N, Imamura Y, Hes O, Kawada T, Nakayama K. Imprint cytologic features in renal cell carcinoma associated with Xp11.2 translocation/TFE3 gene fusion in an adult: a case report. Acta Cytol. 2009;53:693–7.
37. Mansouri D, Dimet S, Couanet D, Terrier-Lacombe MJ, Vasiliu V, Khalifa C, et al. Renal cell carcinoma with an Xp11.2 translocation in a 16–year–old girl: a case report with cytological features. Diagn Cytopathol. 2006;11:757–60.
38. Srigley J. Mucinous tubular and spindle cell carcinoma. In: Eble JN, Sauter G, Epstein JI, Sesterhenn IA, editors. Pathology and genetics of tumors of the urinary system and male genital organs world health organization classification of tumors. Lyon: ARC Press; 2004. p. 40.
39. Parwani AV, Husain AN, Epstein JI, Beckwith JB, Argani P. Low–grade myxoid renal epithelial neoplasms with distal nephron differentiation. Hum Pathol. 2001;32:506–12.
40. MacLennan GT, Farrow GM, Bostwick DG. Low–grade collecting duct carcinoma of the kidney: report of 13 cases of low–grade mucinous tubulocystic renal carcinoma of possible collecting duct origin. Urology. 1997;50:679–84.
41. Ortega JA, Solano JG, Perez-Guillermo M. Cytologic aspect of mucinous tubular and spindle–cell renal carcinoma in fine–needle aspirates. Diagn Cytopathol. 2006;34:660–2.
42. Owens CL, Argani P, Ali SZ. Mucinous tubular and spindle cell carcinoma of the kidney: cytopathologic findings. Diagn Cytopathol. 2007;35:593–6.
43. Marks-Jones DA, Zynger DL, Parwani AV, Cai G. Fine needle aspiration biopsy of renal mucinous tubular and spindle cell carcinoma: report of two cases. Diagn Cytopathol. 2009;38:51–5.
44. Sun W, McGregor DK, Ordonez NG, Ayala AG, Caraway NP. Fine needle aspiration cytology of a low grade myxoid renal epithelial neoplasm: a case report. Acta Cytol. 2005;49:525–9.
45. Srigley JR, Eble JN. Collecting duct carcinoma of kidney. Semin Diagn Pathol. 1998;15:54–67.
46. Layfield LJ. Fine–needle aspiration biopsy of renal collecting duct carcinoma. Diagn Cytopathol. 1994;11:74–8.
47. Ono K, Nishino E, Nakamine H. Renal collecting duct carcinoma. Report of a case with cytologic findings on fine needle aspiration. Acta Cytol. 2000;44:380–4.
48. Albadine R, Schultz L, Illei P, Ertoy D, Hicks J, Sharma R, et al. PAX8 (+)/p63 (−) immunostaining pattern in renal collecting duct carcinoma (CDC): a useful immunoprofile in the differential diagnosis of CDC versus urothelial carcinoma of upper urinary tract. Am J Surg Pathol. 2010;34:965–9.
49. Hunter S, Samir A, Eisner B, Gervais D, Maher M, Hahn P, et al. Diagnosis of renal lymphoma by percutaneous image guided biopsy: experience with 11 cases. J Urol. 2006;176:1952–6; discussion 6.
50. Lin X. Cytomorphology of clear cell papillary renal cell carcinoma. Cancer Cytopathol. 2017;125(1):48–54.
51. Truong LD, Caraway N, Ngo T, Laucirica R, Katz R, Ramzy I. Renal lymphoma. The diagnostic and therapeutic roles of fine–needle aspiration. Am J Clin Pathol. 2001;115:18–31.
52. Balachandran I, Walker JW Jr, Broman J. Fine needle aspiration cytology of ALK1(−), CD30+ anaplastic large cell lymphoma post renal transplantation: a case report and literature review. Diagn Cytopathol. 2010;38:213–6.
53. Hollmann TJ, Hornick JL. INI1–deficient tumors: diagnostic features and molecular genetics. Am J Surg Pathol. 2011;35:e47–63.
54. Katz RL, Shirkhoda A. Diagnostic approach to incidental adrenal nodules in the cancer patient. Results of a clinical, radiologic, and fine–needle aspiration study. Cancer. 1985;55:1995–2000.
55. Stelow EB, Debol SM, Stanley MW, Mallery S, Lai R, Bardales RH. Sampling of the adrenal glands by endoscopic ultrasound–guided fine–needle aspiration. Diagn Cytopathol. 2005;33:26–30.
56. Eloubeidi MA, Black KR, Tamhane A, Eltoum IA, Bryant A, Cerfolio RJ. A large single–center experience of EUS–guided FNA of the left and right adrenal glands: diagnostic utility and impact on patient management. Gastrointest Endosc. 2010;71:745–53.
57. Gupta N, Arora SK, Rajwanshi A, Nijhawan R, Srinivasan R. Histoplasmosis: cytodiagnosis and review of literature with special emphasis on differential diagnosis on cytomorphology. Cytopathology. 2010;21:240–4.
58. de Agustin P, Lopez-Rios F, Alberti N, Perez-Barrios A. Fine–needle aspiration biopsy of the adrenal glands: a ten–year experience. Diagn Cytopathol. 1999;21:92–7.
59. Fassina AS, Borsato S, Fedeli U. Fine needle aspiration cytology (FNAC) of adrenal masses. Cytopathology. 2000;11:302–11.
60. Dusenbery D, Dekker A. Needle biopsy of the adrenal gland: retrospective review of 54 cases. Diagn Cytopathol. 1996;14:126–34.
61. Lumachi F, Borsato S, Brandes AA, Boccagni P, Tregnaghi A, Angelini F, et al. Fine-needle aspiration cytology of adrenal masses in noncancer patients: clinicoradiologic and histologic correlations in functioning and nonfunctioning tumors. Cancer. 2001;93:323–9.
62. Haseganu LE, Diehl DL. Left adrenal gland hemorrhage as a complication of EUS-FNA. Gastrointest Endosc. 2009;69:e51–2.
63. Jimenez-Heffernan JA, Vicandi B, Lopez-Ferrer P, Gonzalez-Peramato P, Perez-Campos A, Viguer JM. Cytologic features of pheochromocytoma and retroperitoneal paraganglioma: a morphologic and immunohistochemical study of 13 cases. Acta Cytol. 2006;50:372–8.
64. Voravud N, Shin DM, Dekmezian RH, et al. Implantation metastasis of carcinoma after percutaneous fine-needle aspiration biopsy. Chest. 1992;102:313–5.
65. Wu HH, Cramer HM, Kho J, Elsheikh TM. Fine needle aspiration cytology of benign adrenal cortical nodules. A comparison of cytologic findings with those of primary and metastatic adrenal malignancies. Acta Cytol. 1998;42:1352–8.

66. Ren R, Guo M, Sneige N, Moran CA, Gong Y. Fine-needle aspiration of adrenal cortical carcinoma: cytologic spectrum and diagnostic challenges. Am J Clin Pathol. 2006;126:389–98.
67. McNicol AM. Update on tumours of the adrenal cortex, phaeochromocytoma and extra–adrenal paraganglioma. Histopathology. 2011;58:155–68.
68. Saboorian MH, Katz RL, Charnsangavej C. Fine needle aspiration cytology of primary and metastatic lesions of the adrenal gland. A series of 188 biopsies with radiologic correlation. Acta Cytol. 1995;39:843–51.
69. Lam KY, Lo CY. Metastatic tumours of the adrenal glands: a 30–year experience in a teaching hospital. Clin Endocrinol. 2002;56:95–101.
70. Wadih GE, Nance KV, Silverman JF. Fine–needle aspiration cytology of the adrenal gland. Fifty biopsies in 48 patients. Arch Pathol Lab Med. 1992;116:841–6.